Eur. Phys. J. C 54, 129–147 (2008)
DOI 10.1140/epjc/s10052-007-0503-4

THE EUROPEAN PHYSICAL JOURNAL C

Regular Article – Theoretical Physics

Exploring the di-photon decay of a light Higgs boson in the MSSM with explicit CP violation

S. Hesselbach[1,a], S. Moretti[1,2,b], S. Munir[1,c], P. Poulose[1,3,d]

[1] School of Physics and Astronomy, University of Southampton, Highfield, Southampton SO17 1BJ, UK
[2] Laboratoire de Physique Théorique, Université Paris-Sud, 91405 Orsay Cedex, France
[3] Physics Department, IIT Guwahati, Assam, 781039, India

Received: 31 August 2007 / Revised version: 30 November 2007 /
Published online: 26 January 2008 –

Abstract. The di-photon decay channel of the lightest Higgs boson is considered as a probe to explore CP violation in the minimal supersymmetric standard model (MSSM). The scalar/pseudo-scalar mixing is considered along with CP violation entering through the Higgs–sfermion–sfermion couplings, with and without light sparticles. The impact of a light stop on the decay width and branching ratio (BR) is established through a detailed study of the amplitude of the process $H_1 \to \gamma\gamma$. The other sparticles have little influence even when they are light. With a suitable combination of other MSSM parameters, a light stop can change the BR by more than 50% with a CP-violating phase $\phi_\mu \sim 90^\circ$, while the change is almost nil with a heavy stop.

1 Introduction

Despite its success in describing the physics of elementary particles there are strong hints that the standard model (SM) is only an effective theory valid up to the TeV range, and new physics is needed to explain particle dynamics (much) beyond this energy scale. Among many others, supersymmetry (SUSY) is one of the most favoured scenarios and will be explored in all possible ways at the upcoming large hadron collider (LHC) at CERN. Furthermore, one of the main tasks of the LHC is the search for Higgs bosons, i.e. the determination of the underlying mechanism of electro-weak symmetry breaking (EWSB). Precision measurements at CERN LEP and SLAC SLC prefer a light Higgs particle, which is indeed predicted in SUSY models. The scalar potential of the MSSM conserves CP at tree level (for reviews, see [1–3]), because SUSY imposes an additional (holomorphic) symmetry on the Higgs sector of a general two-Higgs doublet model that enforces flavour conservation in tree-level neutral currents and the absence of CP-violating scalar/pseudo-scalar mixing in the Born approximation. Beyond tree level, the CP invariance of the Higgs potential may in principle be spontaneously broken by radiative corrections when the vacuum expectation values (VEVs) of the two Higgs doublets develop a relative phase [4, 5]. According to the Georgi–Pais theorem [6] though, this type of CP violation requires a very light Higgs state, which is essentially ruled out by experiment [7–9].

On the other hand many new MSSM parameters can well be complex and thus explicitly break CP invariance. Beyond the Born approximation these new CP-violating phases induce CP violation also in the Higgs sector [5, 10]. The possibly complex parameters include

(i) the higgsino mass term μ,
(ii) the soft SUSY-breaking gaugino masses M_a ($a = 1, 2, 3$),
(iii) the soft bilinear term $B\mu$ and
(iv) the soft trilinear Yukawa couplings A_f of the Higgs particles to scalar fermions of flavour f.

In general, all of these new phases are independent. However, when imposing universality conditions at a unification scale $M_{\rm GUT}$ all the three gaugino masses M_a have a common phase, as well as all the trilinear couplings A_f have another common phase, i.e., four independent phases remain: those of μ, $B\mu$, M_a and A_f. Furthermore, the two U(1) symmetries of the conformal-invariant part of the MSSM may be employed to re-phase one of the Higgs doublet fields and the gaugino fields such that M_a and $B\mu$ are real [10, 11]. In this paper we will work within this setup with two independent physical phases, which we take to be $\arg(\mu) = \phi_\mu$ and $\arg(A_f) = \phi_{A_f}$.

The new CP-violating phases in the MSSM are severely constrained by bounds on the electric dipole moments (EDMs) of electron, neutron and the Hg atom. In order to avoid problems with phases associated with the sfermions of the first and second generations one may deviate from exact universality and consider A_f to be diagonal in flavour

[a] e-mail: s.hesselbach@hep.phys.soton.ac.uk
[b] e-mail: stefano@hep.phys.soton.ac.uk
[c] e-mail: shobig@hep.phys.soton.ac.uk
[d] e-mail: poulose@hep.phys.soton.ac.uk, poulose@iitg.ernet.in

space with vanishing first and second generation couplings [12]. In general, the constraints are rather model dependent and there have been several suggestions [13–30] to evade these constraints allowing large CP-violating phases of $\mathcal{O}(1)$. One possibility is to arrange for partial cancellations among various contributions to the EDMs [19–24]. In this scenario, it has recently been pointed out that for large trilinear scalar couplings A_f, phases $\phi_\mu \sim \mathcal{O}(1)$ can be compatible with the EDM bounds [25]. Another option is to make the first two generations of scalar fermions rather heavy, of order of a few TeV, so that the one-loop EDM constraints are automatically evaded; however, two-loop contributions of third generation scalar fermions may still be large [12]. (A detailed analysis of the so-called CPX scenario with very heavy first and second generations squarks is available in [26].) As a matter of fact, one can consider so-called effective SUSY models [27–29] where decoupling of the first and second generation sfermions is invoked to solve the SUSY flavour changing neutral current (FCNC) and CP problems without spoiling the naturalness condition. Furthermore, the restrictions on the phases may also disappear if lepton flavour violating terms in the MSSM Lagrangian are included [30]. In conclusion, this means that large phases cannot be ruled out and therefore we analyse the full range $0° \leq (\phi_\mu, \phi_A) \leq 180°$ in the following.

The CP-violating SUSY phases can in principle be determined directly in SUSY particles production and decay at high energy colliders [10, 31–45] or indirectly via their radiative effects on the Higgs sector [10, 34]. Here we focus on the di-photon decay mode, $H_1 \to \gamma\gamma$, of the lightest neutral Higgs boson H_1, which involves direct, i.e. leading, effects of the SUSY phases through couplings of the H_1 to SUSY particles in the loops (see Fig. 1) as well as indirect, i.e. sub-leading, effects through the scalar/pseudo-scalar mixing yielding the Higgs mass eigenstate H_1. The di-photon decay mode is important for the study of CP-violating effects in the MSSM Higgs sector for two reasons. On the one hand, it is the most promising channel for the discovery of a light neutral Higgs state with mass between 80 and 130 GeV at the LHC [46, 47]. On the other hand, the coupling strength of the dominant CP-violating terms of the di-photon decay width, which depend on μ and A_f

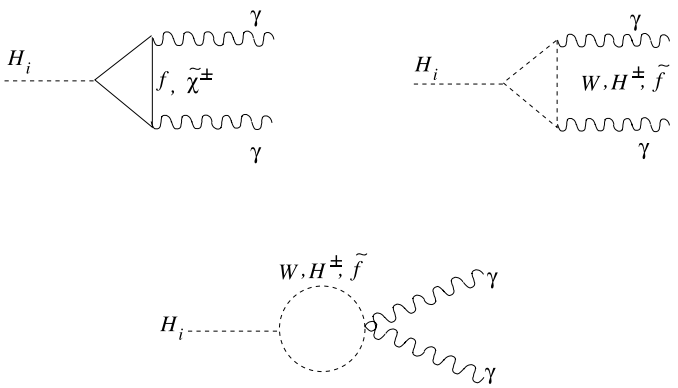

Fig. 1. Diagrams for Higgs decay into $\gamma\gamma$ pairs in the CP-violating MSSM: $f \equiv t, b, \tau$; $\tilde{f} \equiv \tilde{t}_{1,2}, \tilde{b}_{1,2}, \tilde{\tau}_{1,2}$

(with $f = b, t, \tau$, hereafter) is of the same order, $\mathcal{O}(\alpha^3)$, as that of the CP-conserving ones.

The entire $gg/qq \to H_1 \to \gamma\gamma$ process can be factorised exactly into three parts: the production process, the Higgs propagator and the decay channel. (Herein, we will adopt this factorisation in the narrow width approximation, thereby neglecting small corrections of $\mathcal{O}(\Gamma_{H_1}/M_{H_1})$, as $\Gamma_{H_1} \ll M_{H_1}$ for a light Higgs state.) In this process, the effects of CP violation can occur through the aforementioned couplings in the production, through a possible mixing of Higgs states at one loop and above in the propagator and through the same couplings in the decay. CP violation in the production of a Higgs state in the gluon–gluon fusion process at hadron colliders was studied first by [48, 49], choosing a parameter space region that is not sensitive to the CP mixing of the Higgs states, and later by [32, 51], including the presence of CP mixing of the Higgs states.[1] The effects of CP mixing in the propagator are discussed separately but in great detail in [38, 39]. A detailed study of the other MSSM Higgs decay channels in the presence of CP violation can be found in [31–39, 50–56][2].

The results of a random parameter space scan to understand the general behaviour of $\mathrm{BR}(H_1 \to \gamma\gamma)$ for non-zero ϕ_μ values are reported in [60]. It has been seen that about 50% deviations are possible for M_{H_1} around 104 GeV for $\phi_\mu = 100°$, and an average of 30% deviation occurs over the mass range 90–130 GeV. Masses around and below 110 GeV show a decrease in the BR for non-zero ϕ_μ values, while masses above this value show an increase. Certain individual parameter space points were also discussed in [60]. Specifically, $|A_f| = 1.5$ TeV, $|\mu| = 1$ TeV, $\tan\beta = 20$ was considered as a benchmark scenario. Then, by choosing (a) $M_{\tilde{U}_3} = 1$ TeV and (b) $M_{\tilde{U}_3} = 250$ GeV, it was demonstrated that the light stop $\tilde{t}_1$ has a strong impact on our decay mode, through the μ and the trilinear couplings A_f, which is quite different from the effects due only to the (one-loop) change of the $H_1W^+W^-$ coupling [51]. In [60], it was also noticed that the effect of a light $\tilde{t}_1$ is in the opposite direction as compared to that due to modifications of the H_1 coupling to the SM particles.

In this article we will consolidate the results of [60] by a detailed discussion of the following points.

- The Higgs mixing matrix elements are discussed in detail showing the changes in mixing as the phase ϕ_μ is varied.
- The decay amplitudes due to individual (s)particles in the loops are presented in detail and the real and imaginary parts of the scalar and pseudo-scalar contributions are given separately. We will see that this unambiguously shows that a light stop contribution is comparable to the SM one, while the other sparticles have negligible effects even in scenarios when they are light.
- Compared to [60], where only one particular value was considered for $\tan\beta$, $|\mu|$ and $|A_f|$, we present here results

[1] CP violation in vector boson associated production (VH_i) is studied by [52].

[2] Here all these decay modes have been studied inclusively. A discussion of CP violation in exclusive four lepton final states via gauge boson decays can be found in [57–59].

with the four different values $\tan\beta = 2,\ 5,\ 20,\ 50$, the two different values $|\mu| = 0.5, 1$ TeV and the two different values $|A_f| = 0.5, 1.5$ TeV.

We postpone the full analysis of $gg/qq \to H_1 \to \gamma\gamma$ to a forthcoming publication [61]. The outline of this paper is as follows. In Sect. 2 the CP mixing in the Higgs sector is explained in more detail. In Sect. 3 we analyse the phase dependence of $H_1 \to \gamma\gamma$. We conclude in Sect. 4.

2 Higgs mixing in the CP-violating MSSM

In the Higgs sector of the MSSM with explicit CP violation the CP-violating phases introduce non-vanishing off-diagonal mixing terms in the neutral Higgs mass matrix, which in the weak basis (ϕ_1, ϕ_2, a), where $\phi_{1,2}$ are the CP-even states and a is the CP-odd state, may schematically be written as [10, 34, 50, 62, 63]

$$\mathcal{M}_H^2 = \begin{pmatrix} \mathcal{M}_S^2 & \mathcal{M}_{SP}^2 \\ \mathcal{M}_{PS}^2 & \mathcal{M}_P^2 \end{pmatrix}. \tag{1}$$

Here, $\mathcal{M}_S^2$ is a 2×2 matrix describing the transition between the CP-even states, $\mathcal{M}_P^2$ gives the mass of the CP-odd state, while $\mathcal{M}_{PS}^2 = (\mathcal{M}_{SP}^2)^{\mathrm{T}}$ (a 1×2 matrix) describes the mixing between the CP-even and CP-odd states. The mixing matrix elements are typically proportional to

$$\mathcal{M}_{SP}^2 \propto \mathrm{Im}(\mu A_f) \tag{2}$$

and dominated by loops involving the top squarks. As a result, the neutral Higgs bosons of the MSSM no longer carry any definite CP-parities. Rotation from the EW states to the mass eigenvalues,

$$(\phi_1, \phi_2, a)^{\mathrm{T}} = O(H_1, H_2, H_3)^{\mathrm{T}},$$

is now carried out by a 3×3 real orthogonal matrix O, such that

$$O^{\mathrm{T}} \mathcal{M}_H^2 O = \mathrm{diag}\big(M_{H_1}^2, M_{H_2}^2, M_{H_3}^2\big) \tag{3}$$

with $M_{H_1} \le M_{H_2} \le M_{H_3}$. As a consequence, it is now appropriate to parametrise the Higgs sector of the CP-violating MSSM in terms of the mass of the charged Higgs boson, $M_{H^\pm}$, as the latter remains basically unaffected. (For a detailed formulation of the MSSM Higgs sector with explicit CP violation, see [10, 50].)

3 $H_1 \to \gamma\gamma$ in the CP-violating MSSM

A Higgs boson in the MSSM decays at one-loop level into two photons through loops of fermions, sfermions, $W^\pm$ bosons, charged Higgs bosons and charginos; see Fig. 1. The analytical expressions for the respective amplitude along with relevant couplings in the CP-violating MSSM can be found in [64] and references therein. The amplitude has the form

$$\mathcal{M}_{\gamma\gamma H_i} = -\frac{\alpha M_{H_i}^2}{4\pi v}\left\{ S_i^\gamma(M_{H_i})(\epsilon_{1\perp}^* \cdot \epsilon_{2\perp}^*) - P_i^\gamma(M_{H_i}) \frac{2}{M_{H_i}^2} \langle \epsilon_1^* \epsilon_2^* k_1 k_2 \rangle \right\}, \tag{4}$$

where $k_{1,2}$ are the momenta of the two photons and $\epsilon_{1,2}$ are their polarisation vectors, which are conveniently written as $\epsilon_{r\perp}^\mu = \epsilon_r^\mu - 2k_r^\mu (k_s \cdot \epsilon_r)/M_{H_i}^2$ $(r \neq s)$ and where $\langle \epsilon_1 \epsilon_2 k_1 k_2 \rangle \equiv \varepsilon_{\mu\nu\rho\sigma} \epsilon_1^\mu \epsilon_2^\nu k_1^\rho k_2^\sigma$. S_i^γ and P_i^γ are given by (retaining only the dominant loop contributions)

$$\begin{aligned} S_i^\gamma(M_{H_i}) = 2 &\sum_{f=t,b,\tau,\tilde{\chi}_1^\pm,\tilde{\chi}_2^\pm} N_C Q_f^2 g_f g^S_{H_i f\bar{f}} \frac{v}{m_f} F_{sf}(\tau_{if}) \\ &- \sum_{\tilde{f}_j=\tilde{t}_1,\tilde{t}_2,\tilde{b}_1,\tilde{b}_2,\tilde{\tau}_1,\tilde{\tau}_2} N_C Q_f^2 g_{H_i \tilde{f}_j^* \tilde{f}_j} \frac{v^2}{2m_{\tilde{f}_j}^2} F_0(\tau_{i\tilde{f}_j}) \\ &- g_{H_i WW} F_1(\tau_{iW}) - g_{H_i H^+ H^-} \frac{v^2}{2M_{H^\pm}^2} F_0(\tau_{iH^\pm}), \\ P_i^\gamma(M_{H_i}) = 2 &\sum_{f=t,b,\tau,\tilde{\chi}_1^\pm,\tilde{\chi}_2^\pm} N_C Q_f^2 g_f g^P_{H_i f\bar{f}} \frac{v}{m_f} F_{sf}(\tau_{if}). \end{aligned}$$

For the expressions of the various couplings (the g) and form factors ($F(\tau)$) we refer to [64]. Then the partial decay width is given by

$$\Gamma(H_i \to \gamma\gamma) = \frac{M_{H_i}^3 \alpha^2}{256\pi^3 v^2}\left[\big|S_i^\gamma(M_{H_i})\big|^2 + \big|P_i^\gamma(M_{H_i})\big|^2 \right]. \tag{5}$$

The decay mode $H_i \to \gamma\gamma$, $i = 1, 2, 3$, is discussed by [51] along with Higgs production through gluon–gluon fusion. However, that study was confined to MSSM parameter space regions with suitably heavy sparticles $\tilde{f}$ and $\tilde{\chi}^\pm$, where CP-violating effects are only due to the changed SM particle (especially $W^\pm$) couplings to the H_1 and effects of sparticles in the triangle loops entering the decay amplitude are negligible. Here we examine the complementary region of MSSM parameter space with light sparticles, so that they contribute substantially to the latter. In particular, we will show that, in the presence of non-trivial CP-violating phases, regions of MSSM parameter space exist where the couplings of the Higgs bosons to all sparticles in the decay loops are strongly modified with respect to the CP-conserving MSSM, thereby inducing dramatic changes on the $H_1 \to \gamma\gamma$ width and BR.

We have analysed the Higgs decay widths and BRs with the publicly available FORTRAN code CPSuperH [64] version 2, which is based on the results obtained in [31–35] and the most recent renormalisation group improved effective-potential approach, which includes dominant higher-order logarithmic and threshold corrections, b-quark Yukawa coupling re-summation effects and Higgs boson pole-mass shifts [50, 65]. CPSuperH calculates the mass spectrum and

decay widths of the neutral and charged Higgs bosons in the general CP-violating MSSM including the phases of A_f and μ. Furthermore, it computes all the couplings of the neutral Higgs bosons $H_{1,2,3}$ and the charged Higgs boson $H^{\pm}$ to SM particles and their superpartners.

The open non-SM parameters of the model now include the higgsino mass $|\mu|$, its phase ϕ_μ, the charged Higgs mass $M_{H^\pm}$, the soft gaugino masses M_a, the soft sfermion masses of the third generation $M_{(\tilde{Q}_3,\tilde{U}_3,\tilde{D}_3,\tilde{L}_3,\tilde{E}_3)}$, the (unified) soft trilinear coupling of the third generation $|A_f|$ and its phase ϕ_{A_f}.

In our analysis we fix the following SUSY parameters:

- $M_1 = 100$ GeV, $M_2 = 1$ TeV, $M_3 = 1$ TeV, and
- $M_{\tilde{Q}_3} = M_{\tilde{D}_3} = M_{\tilde{L}_3} = M_{\tilde{E}_3} = M_{\rm SUSY} = 1$ TeV,

whereas the following parameters are varied:

- $\tan\beta = 2, 5, 20, 50$,
- $|A_f| = 500$ GeV, 1.5 TeV,
- $\phi_{A_f} = 0^\circ$ (whereas the CP-violating effects in the sparticle sector depend on both ϕ_μ and ϕ_{A_f}, the leading CP-violating effects on the Higgs sector, as stated above, are proportional to $\mathrm{Im}(\mu A_f)$, and so we opted to fix ϕ_{A_f} to 0° and varied only ϕ_μ),
- $|\mu| = 500$ GeV, 1 TeV,
- $\phi_\mu = 0$–180°,
- $M_{H^+} = 100$–300 GeV,
- $M_{\tilde{U}_3} = 250$ GeV (case with light $\tilde{t}_1$) and $M_{\tilde{U}_3} = 1$ TeV (case with no light sfermion).

For this analysis, threshold corrections induced by the exchange of gluinos and charginos in the Higgs–quark–antiquark vertices [66–75] were not included. While these corrections may change the actual values of the width and BR, we expect them to be the same for the CP-conserving and CP-violating cases. The situation will be different if ϕ_3, the phase of M_3, could be non-zero. As mentioned in the introduction, we have considered the case of a common phase for the gaugino mass terms, which is rotated away, making M_a ($a = 1, 2, 3$) real.

The mass of the lightest neutral Higgs boson, M_{H_1}, is sensitive to the value of ϕ_μ chosen. This dependence on

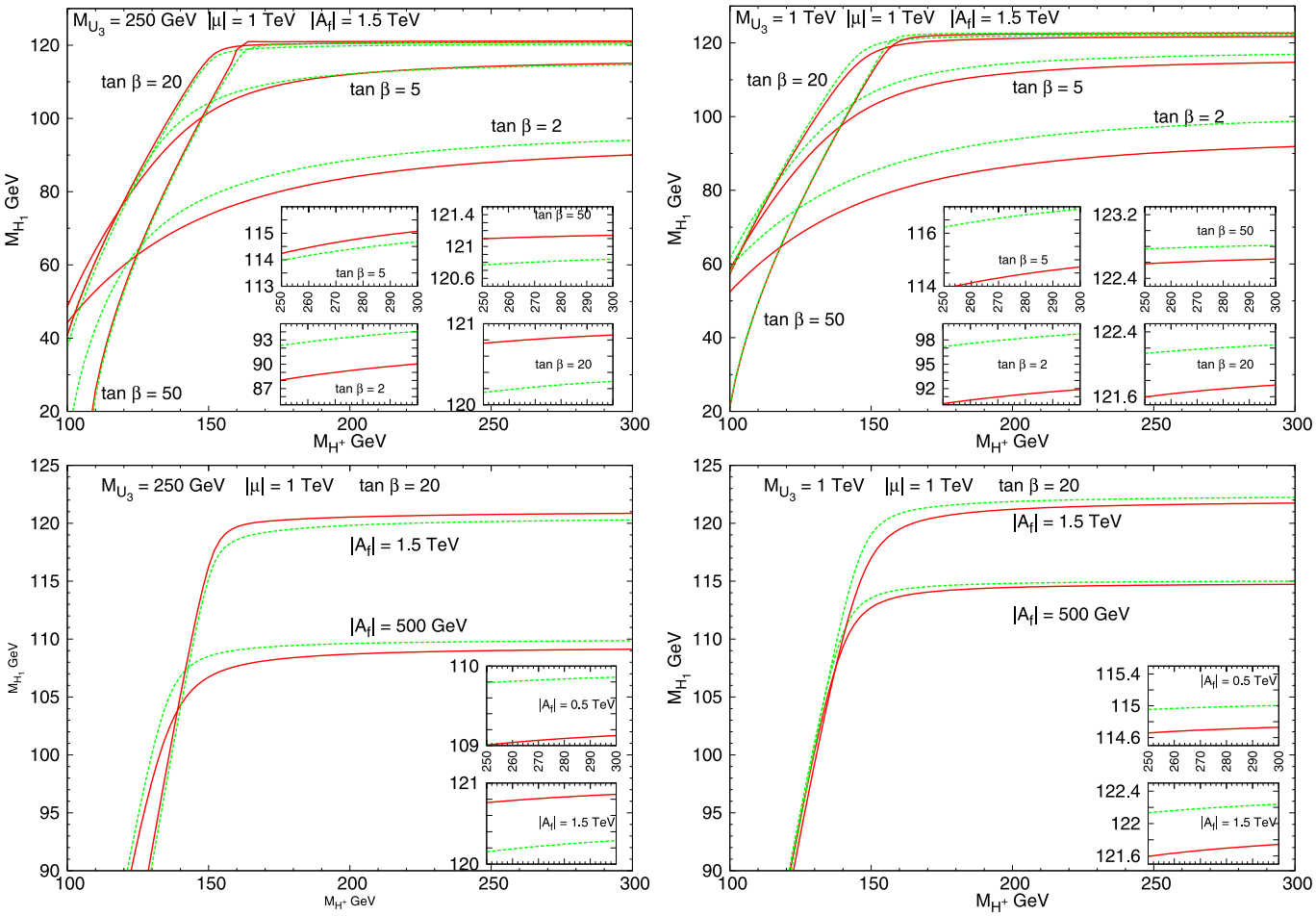

Fig. 2. Mass of the lightest neutral Higgs boson H_1 against M_{H^+} for $\phi_\mu = 0^\circ$ (*solid*, *red line*) and $\phi_\mu = 90^\circ$ (*dashed*, *green line*) with $|A_f| = 1.5$ TeV, $|\mu| = 1$ TeV and different values of $\tan\beta$ (*top row*) and $\tan\beta = 20$, $|\mu| = 1$ TeV and different values of $|A_f|$ (*bottom row*), respectively. In the *left column* a light stop (~ 200 GeV) is present for $M_{\tilde{U}_3} = 250$ GeV and $M_{\tilde{Q}_3} = M_{\rm SUSY} = 1$ TeV, whereas in the *right column* all sparticles are heavy (~ 1 TeV) for $M_{\tilde{U}_3} = M_{\tilde{Q}_3} = M_{\rm SUSY} = 1$ TeV

ϕ_μ along with that on other SUSY parameters is illustrated in Fig. 2, where M_{H_1} is plotted against the charged Higgs mass for $\tan\beta = 2,\ 5,\ 20,\ 50$, $|A_f| = 0.5,\ 1.5$ TeV and $|\mu| = 1$ TeV. Concerning the sparticles in the loop, two cases are considered. The first case comprises a light $m_{\tilde{t}_1} \sim 200$ GeV (corresponding to $M_{\tilde{U}_3} = 250$ GeV and $M_{\tilde{Q}_3} = M_{\rm SUSY} = 1$ TeV), while all other sparticles are heavy, while in the other case $m_{\tilde{t}_1}$ is also taken in the TeV range with $M_{\tilde{U}_3} = M_{\tilde{Q}_3} = M_{\rm SUSY} = 1$ TeV. The top row in Fig. 2 shows the sensitivity of M_{H_1} to $\tan\beta$ for $|\mu| = 1$ TeV and $|A_f| = 1.5$ TeV. While in the low $\tan\beta$ case the mass shift induced by the change in ϕ_μ from 0° to 90° is about 10%, in the case of $\tan\beta = 20$ or above it is about 1% or less. Notice that the relevant parameters here are $|A_f|$ and $|\mu|$, and M_{H_1} is found to increase with increasing $|A_f|$ while its dependence on $|\mu|$ is basically negligible. In the bottom row of Fig. 2 we plot the M_{H_1} dependence on $M_{H^\pm}$ for the two representative values of $|A_f|$, 0.5 and 1.5 TeV, by keeping $\tan\beta = 20$ and $|\mu| = 1$ TeV.

The sudden shift in the dependence of M_{H_1} on M_{H^+} around $M_{H^+} = 150$ GeV is understood in terms of the cross over in the mass eigenstates at that point. We have illustrated this in Fig. 3, where the masses of $H_{1,2,3}$ are plotted against M_{H^+} for $\tan\beta = 20$, $|A_f| = 1.5$ TeV and $|\mu| = 1$ TeV, again with light and heavy stops. The cross over is a reflection of the changing compositions of the CP indefinite mass eigenstates, H_1, H_2 and H_3, with eigenvalues $M_{H_1} < M_{H_2} < M_{H_3}$, in terms of the CP definite gauge eigenstates, ϕ_1, ϕ_2 and a. To explain this in a little more detail, let us denote the mass eigenvalues as m_1, m_2 and m_3, and the corresponding eigenstates as h_1, h_2 and h_3, before ordering them from lightest to heaviest (i.e., h_1 need not be the lightest for all values of M_{H^+}). Of the three mass eigenvalues, two (m_1 and m_2) grow linearly with M_{H^+} with almost the same slope, lying close to each other. In the CP-conserving case one of these is a pseudoscalar, while the other is a scalar. The other eigenvalue (m_3) corresponds to a scalar eigenstate and is more or less independent of M_{H^+}. At $M_{H^+} \sim 150$ GeV all three CP-conserving eigenstates are degenerate with eigenvalues around 120 GeV. In the $M_{H^+} \lesssim 150$ GeV region h_1 is the lightest, while in the $M_{H^+} \gtrsim 150$ GeV region it is h_3 that is the lightest. When we order such that the lightest one is H_1, there is a transition from $H_1 = h_1$ to $H_1 = h_3$ around $M_{H^+} = 150$ GeV. For other values of $\tan\beta$, A_f and μ the situation is very similar, with small shifts in the actual values of M_{H^+} and the degenerate mass where the cross over happens. In the CP-violating case with non-zero value of ϕ_μ, there is mixing between scalar and pseudo-

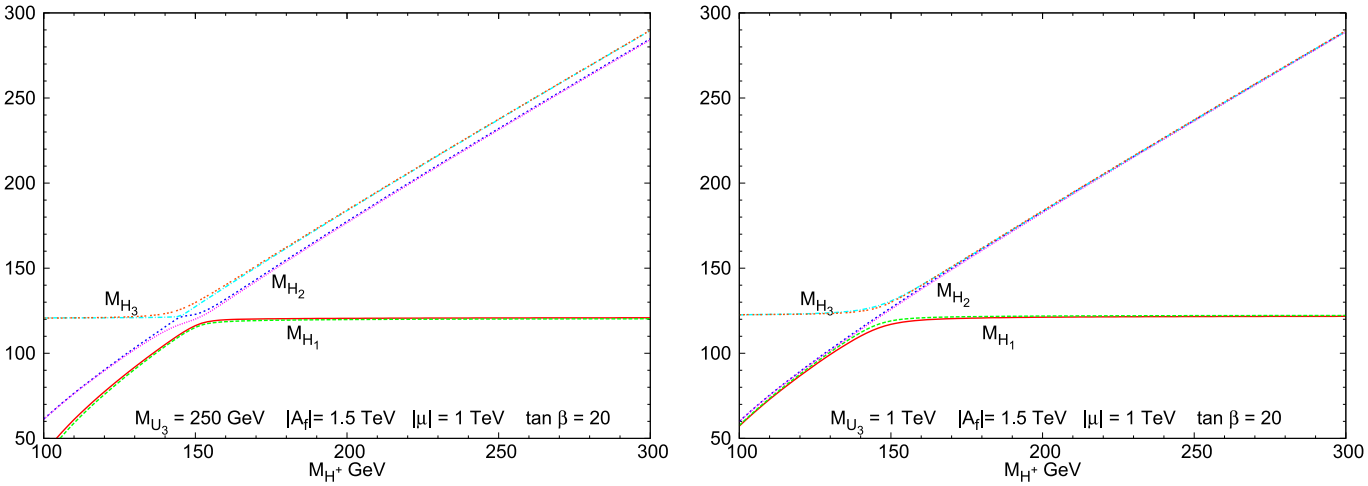

Fig. 3. Mass of $H_{1,2,3}$ against M_{H^+} for $\tan\beta = 20$ showing the cross over at $M_{H^+} \sim 150$ GeV. The *left column* is for $M_{\tilde{U}_3} = 250$ GeV ($m_{\tilde{t}_1} \sim 200$ GeV), while the *right one* is for $M_{\tilde{U}_3} = 1$ TeV (no light sparticle). Both plots are with $|A_f| = 1.5$ TeV, $|\mu| = 1$ TeV. *Red*, *blue* and *cyan curves* represent $\phi_\mu = 0°$, while *green*, *magenta* and *orange curves* correspond to $\phi_\mu = 90°$

Table 1. Selected values of M_{H_i} $(i = 1, 2, 3)$ for $\phi_\mu = 0°$ and $\phi_\mu = 90°$. All SUSY parameters are as in Fig. 3 with $M_{\tilde{U}_3} = 250$ GeV

	$\phi_\mu = 0°$			$\phi_\mu = 90°$		
M_{H^+} (GeV)	M_{H_1} (GeV)	M_{H_2} (GeV)	M_{H_3} (GeV)	M_{H_1} (GeV)	M_{H_2} (GeV)	M_{H_3} (GeV)
100	40.7	61.4	120.7	37.6	61.2	120.7
120	77.4	90.3	120.8	75.8	89.7	121.0
200	120.5	179.8	183.8	119.8	176.7	184.2
250	120.8	232.1	237.3	120.2	231.4	237.6
300	120.9	284.8	289.6	120.3	284.2	289.8

Table 2. Same as Table 1, but with $M_{\tilde{U}_3} = 1$ TeV

	$\phi_\mu = 0^\circ$			$\phi_\mu = 90^\circ$		
M_{H^+} (GeV)	M_{H_1} (GeV)	M_{H_2} (GeV)	M_{H_3} (GeV)	M_{H_1} (GeV)	M_{H_2} (GeV)	M_{H_3} (GeV)
100	57.2	60.0	122.6	57.6	59.8	122.6
120	86.8	89.3	123.1	87.7	88.9	123.0
200	121.2	183.3	183.4	121.9	182.6	183.7
250	121.6	236.9	237.0	122.1	236.4	237.2
300	121.7	289.2	289.3	122.2	288.9	289.5

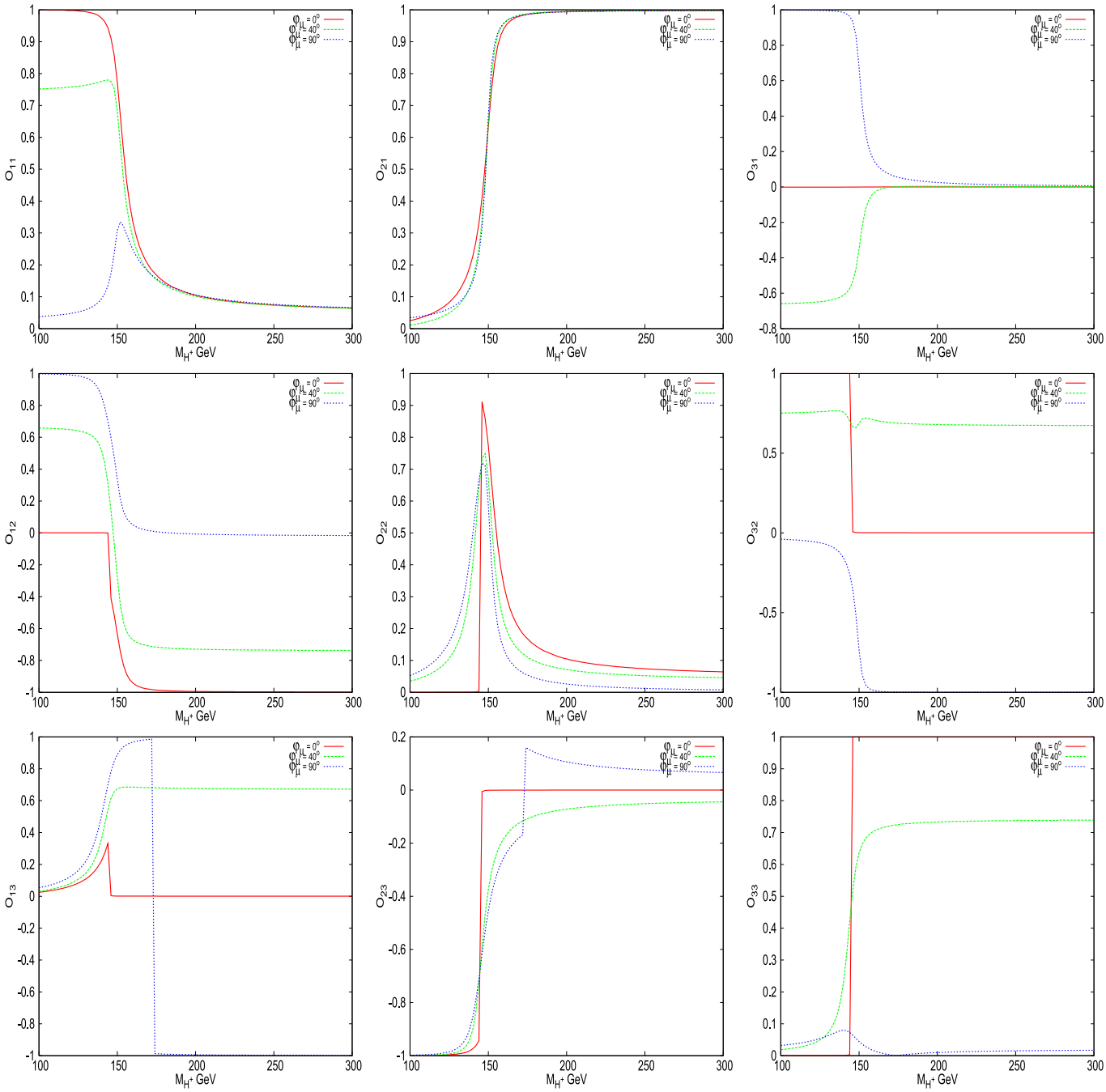

Fig. 4. Mixing matrix elements O_{ij} versus M_{H^+} (such that $H_i = O_{1i}\phi_1 + O_{2i}\phi_2 + O_{3i}a$) with $\tan\beta = 20$, $|A_f| = 1.5$ TeV, $|\mu| = 1$ TeV, $M_{\tilde{Q}_3} = M_{\tilde{D}_3} = M_{\tilde{L}_3} = M_{\tilde{E}_3} = M_{\rm SUSY} = 1$ TeV, $M_{\tilde{U}_3} = 250$ GeV and ϕ_μ as indicated in the plots

scalar states. For larger values of M_{H^+} the lightest Higgs state, H_1, is almost a pure scalar, hence it will not be subject to any CP violation through mixing. The only possible way to have CP violation here is through the $H_1\tilde{f}\tilde{f}^*$ coupling, especially that of the stop quark. We restrict ourselves to regions of parameter space with small M_{H^+}, where the effect of mixing as well as that due to a complex $\phi_{1,2}\tilde{f}\tilde{f}^*$ coupling are present. At large M_{H^+} values, there will be scalar/pseudo-scalar mixing in the heavier Higgs states, H_2 and H_3. (We will not discuss the two heavier states in the present article, though.) Tables 1 and 2 illustrate selected values of the H_1, H_2 and H_3 masses for sample choices of $M_{H^\pm}$ when $\phi_\mu = 0°$ and 90° in the presence of a light stop and otherwise, respectively. Mass shifts can typically be of a few percent, particularly for light Higgs masses in the former case, while they are negligible in the latter.

Next we analyse the Higgs mixing matrix for the parameters $\tan\beta = 20$, $|A_f| = 1.5$ TeV and $|\mu| = 1$ TeV, as an example of a generic pattern over the entire MSSM parameter space. We show the mixing matrix elements in Fig. 4. In the CP-conserving case ($\phi_\mu = 0°$) H_1 is mostly ϕ_1 below $M_{H^+} \sim 150$ GeV and mostly ϕ_2 above it. H_2 is the pseudo-scalar (a) below $M_{H^+} \sim 150$ GeV, while above $M_{H^+} \sim 150$ GeV it is mostly ϕ_1. H_3, on the other hand, is mostly ϕ_2 below $M_{H^+} \sim 150$ GeV and is the pseudo-scalar above this value. Indeed there is some mixing between ϕ_1 and ϕ_2 in the transition region. For the maximum value of $\phi_\mu = 90°$ the lightest (H_1) is mostly the pseudo-scalar below $M_{H^+} \sim 150$ GeV; H_2 is mostly ϕ_1 and H_3 is mostly ϕ_2. Above this region H_1 is mostly ϕ_2, H_2 is mostly a and H_3 is mostly ϕ_1. There is of course some mixing (albeit small) between all the three states (especially in the transition region). For values of ϕ_μ in between 0° and 90° mixing could be large, as demonstrated by the case of $\phi_\mu = 40°$ in Fig. 4. Similar features also occur between $\phi_\mu = 90°$ and 180° (the other CP-conserving value). Concentrating on H_1, the lightest eigenstate, we have plotted the relevant mixing matrix elements in Fig. 5 for the two cases with and without the presence of a light $\tilde{t}_1$, which shows that indeed the mixing is affected by the presence of a light stop.

These CP mixing effects feed into the decay amplitude of (4) through couplings of the H_i to the SM and SUSY particles in the loop (see Fig. 1) at one-loop and tree level, respectively. In Figs. 6–10 we show different contributions to the amplitude of $H_1 \to \gamma\gamma$. Clearly, the SM contribution is dominant in all cases. Among the major contributions within the SM, that from the $W^\pm$ loop is

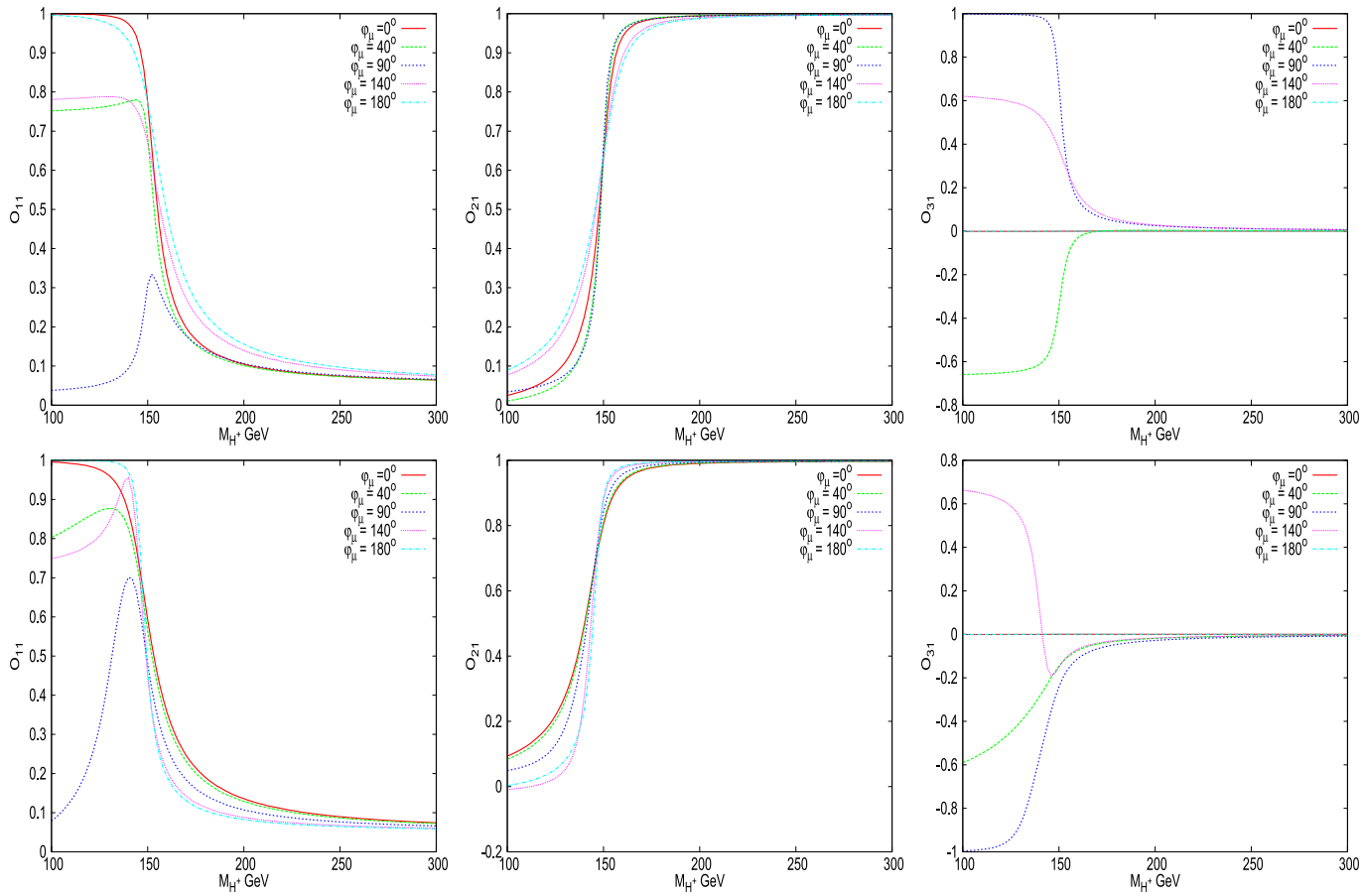

Fig. 5. Mixing matrix elements O_{i1} versus M_{H^+} (such that $H_1 = O_{11}\phi_1 + O_{21}\phi_2 + O_{31}a$) for $\tan\beta = 20$. The *top row* corresponds to $M_{\tilde{U}_3} = 250$ GeV while the *bottom row* corresponds to $M_{\tilde{U}_3} = 1$ TeV. All other parameters are as in Fig. 4

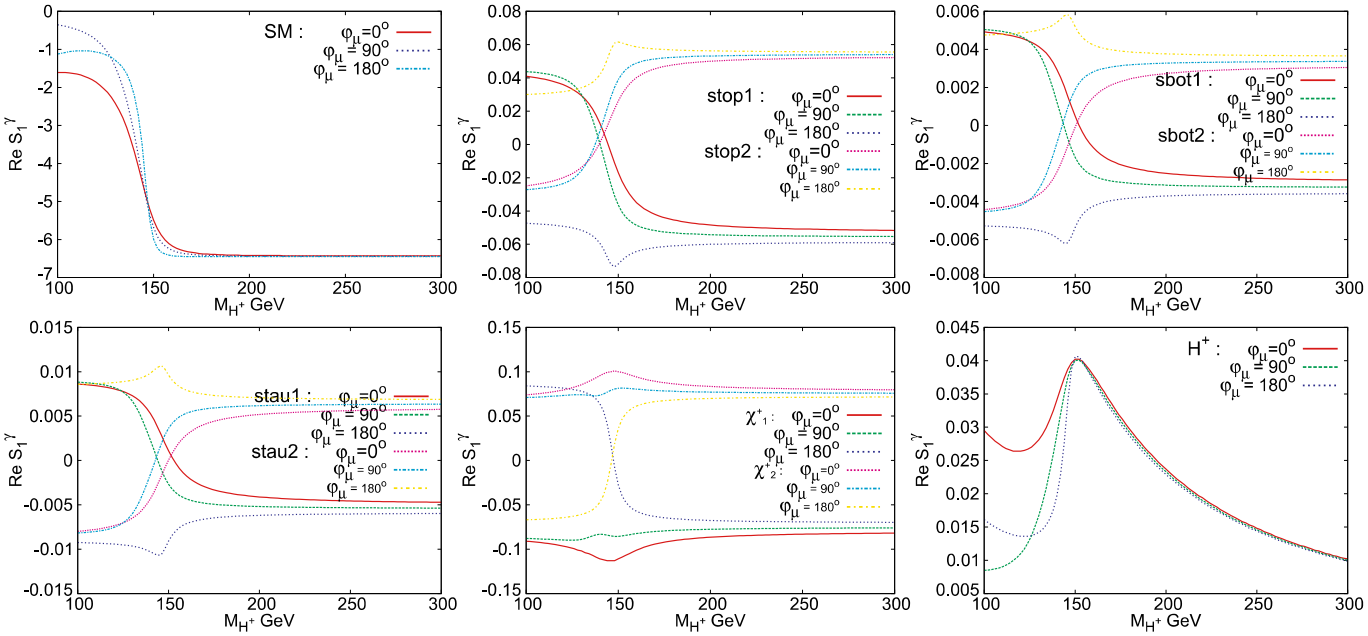

Fig. 6. Different contributions to $\mathrm{Re}(S_1^\gamma)$ against the input parameter M_{H^+} with SUSY parameters as in Fig. 4 and $M_{\tilde{U}_3} = 1$ TeV. *Top row*: (from left) SM, $\tilde{t}_{1,2}$ and $\tilde{b}_{1,2}$. *Bottom row*: (from left) $\tilde{\tau}_{1,2}$, $\tilde{\chi}^+_{1,2}$ and H^+

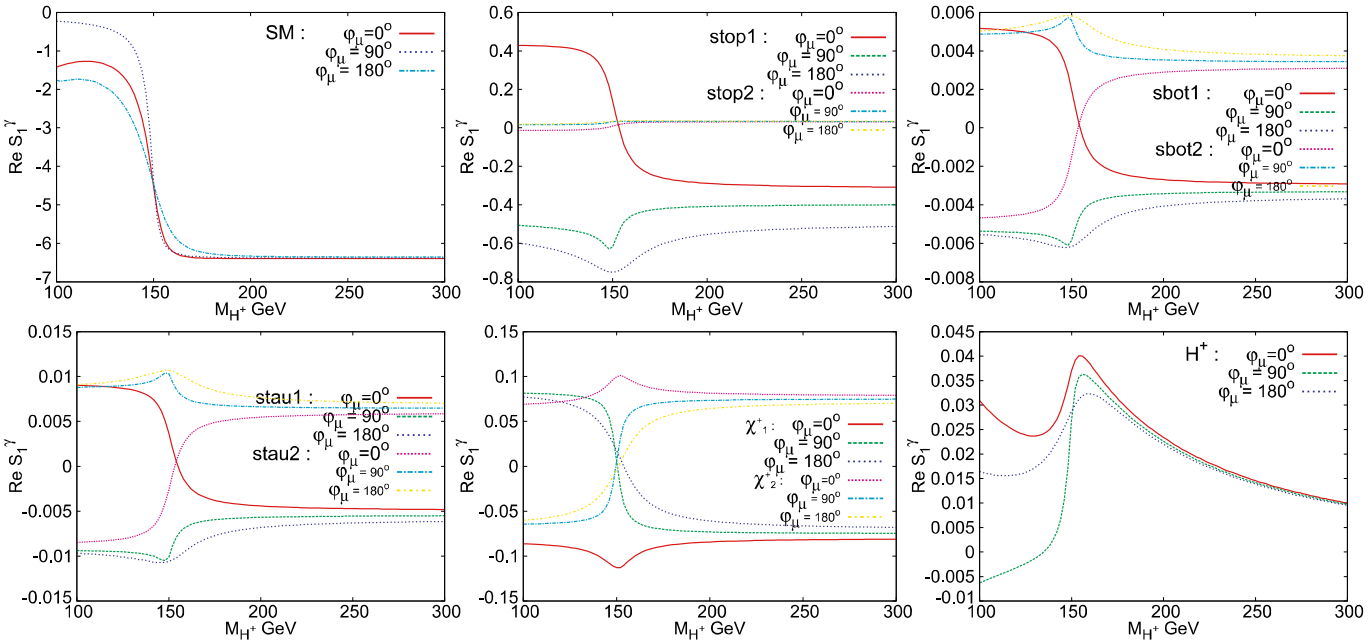

Fig. 7. Different contributions to $\mathrm{Re}(S_1^\gamma)$ against the input parameter M_{H^+} with SUSY parameters as in Fig. 4 and $M_{\tilde{U}_3} = 250$ GeV. *Top row*: (from left) SM, $\tilde{t}_{1,2}$ and $\tilde{b}_{1,2}$. *Bottom row*: (from left) $\tilde{\tau}_{1,2}$, $\tilde{\chi}^+_{1,2}$ and H^+

about 5 times larger than the top quark contribution for the whole range of M_{H^+} (for the chosen set of SUSY parameters), while the bottom quark and tau lepton contributions are about an order of magnitude smaller over the lower range of M_{H^+} (except around 100 GeV) and negligibly small for larger values. Magnitudes of both the $W^\pm$ and top quark contributions grow with M_{H^+}, which is a reflection of the fact that these couplings are proportional to the mixing matrix element O_{21}. When all SUSY states are heavy (Fig. 6), all sparticle (and H^+) contributions to the real part of S_1^γ are two or three orders of magnitude smaller than the SM term. The exception is the chargino contribution, which is at the most 10%. The effect of a light $\tilde{t}_1$ (Fig. 7) enters in two different ways. Firstly, it affects the SM couplings to H_1 through loop corrections (compare the top left plots in Figs. 6 and 7). This is more prominent

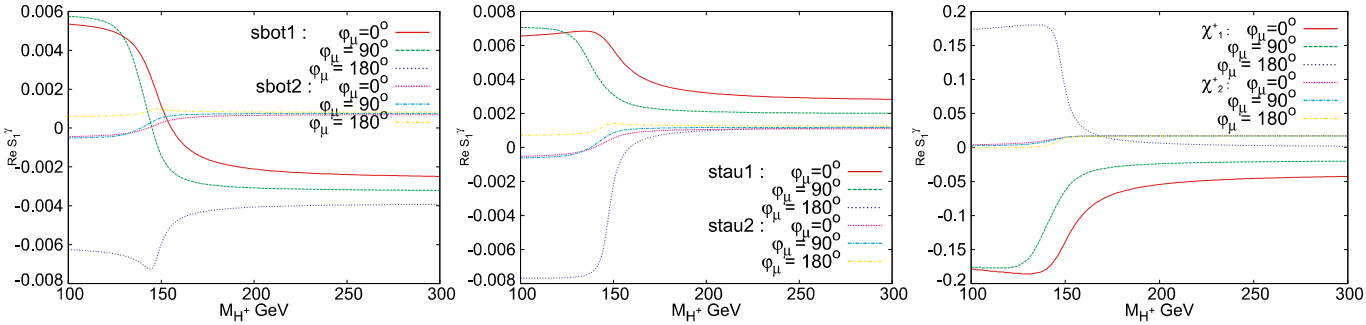

Fig. 8. Contributions to Re (S_1^γ) when the respective sparticle is light. The *left plot* is with $M_{\tilde{D}_3} = 310$ GeV (or $m_{\tilde{b}_1} \sim 300$ GeV), *middle one* is with $M_{\tilde{E}_3} = 310$ GeV (or $M_{\tilde{\tau}_1} \sim 300$ GeV) and the *right one* is with $M_2 = 100$ GeV (or $M_{\chi_1^\pm} \sim 100$ GeV). All other sparticles in the loop are of the order of TeV. The SM contribution in each case remains more or less the same as in Fig. 6 (no light sparticle)

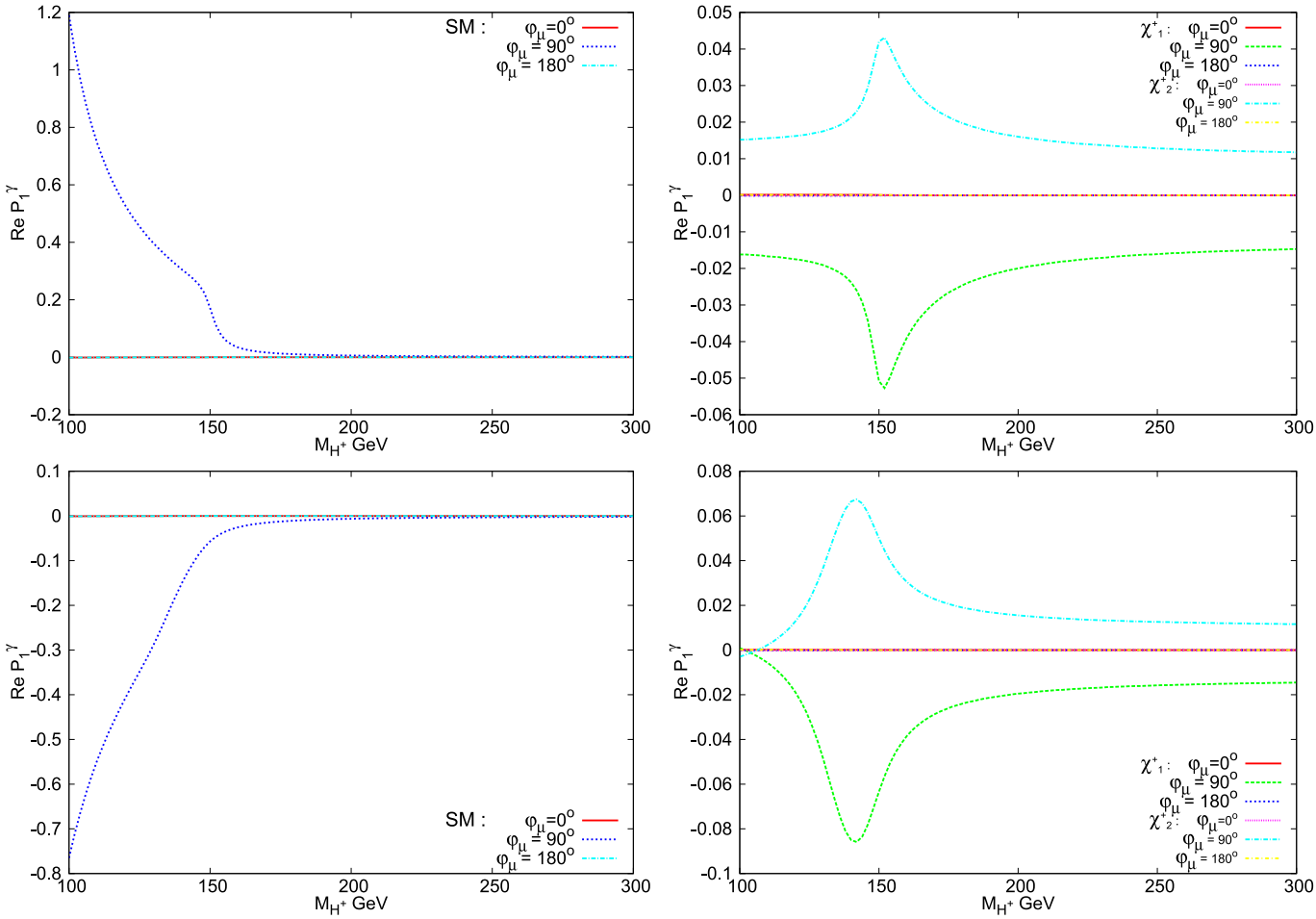

Fig. 9. SM and chargino contributions (as indicated) to Re(P_1^γ). The *top row* corresponds to the case with $M_{\tilde{U}_3} = 250$ GeV and *bottom row* with $M_{\tilde{U}_3} = 1$ TeV. The contributions in CP-conserving parameter points ($\phi_\mu = 0°$ and $\phi_\mu = 180°$) are all consistent with zero

when $\phi_\mu = 180°$. The effects due to change in ϕ_μ are different from the case with no light sparticle. Secondly, the $\tilde{t}_1$ contribution (top middle plot in Fig. 7) is now comparable (about 40% in the CP-conserving case) to that of the SM. Contributions of other sparticles are not changed much going from larger to smaller masses of the respective sparticle as shown in Fig. 8. In Fig. 9 contributions to the real part of P_1^γ are plotted against M_{H^+}. These terms come through the pseudo-scalar component in H_1. Since the squarks, sleptons and the charged Higgs boson do not couple to a, only SM objects and charginos contribute to P_1^γ. For the CP-conserving case it vanishes, as expected. When ϕ_μ is non-zero, H_1 has an a component and there is a non-vanishing P_1^γ, as illustrated by the curve correspond-

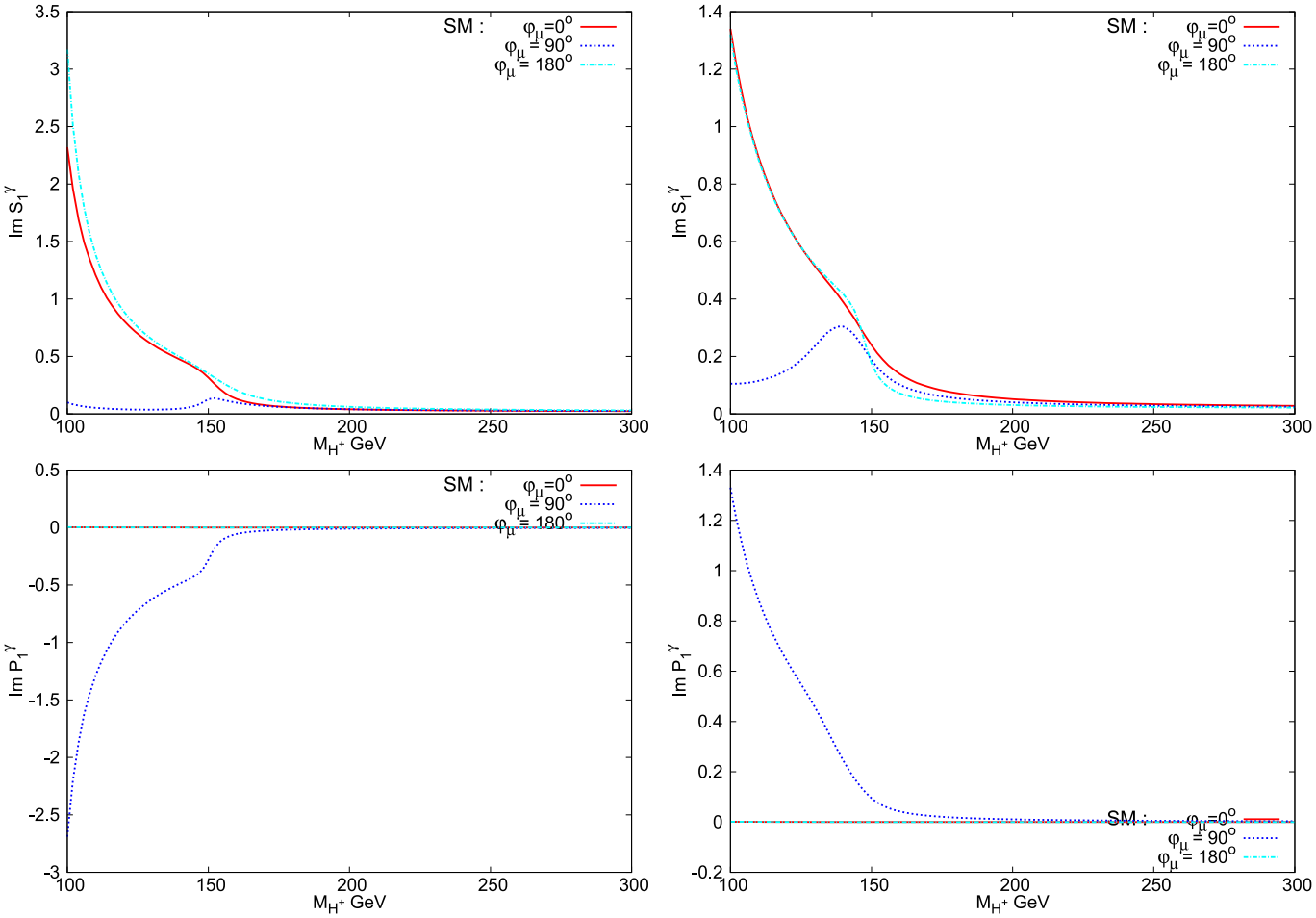

Fig. 10. SM contribution to $\mathrm{Im}(S_1^\gamma)$ (*first row*) and $\mathrm{Im}(P_1^\gamma)$ (*second row*) against the input parameter M_{H^+}, for the case with $M_{\tilde{U}_3} = 250\,\mathrm{GeV}$ (*left column*) and with $M_{\tilde{U}_3} = 1\,\mathrm{TeV}$ (*right column*). Contributions from superparticles are zero

ing to $\phi_\mu = 90°$ in Fig. 9. Figure 10 shows the imaginary parts of S_1^γ and P_1^γ, which are sensitive to the value of ϕ_μ. For the H_1 mass range considered here only the SM contribution is complex. Again, P_1^γ being the contribution from a coupling to the (s)particles, its imaginary part vanishes in the CP-conserving cases. The $H_1 \to \gamma\gamma$ width is not sensitive to the sign of $\mathrm{Im}\, P_1^\gamma$, therefore the difference between the cases of light $\tilde{t}_1$ and no light sparticle is not very dramatic.

From our MSSM parameter space scans, the following generic features on the sensitivity of width and BR to the CP-violating phase, ϕ_μ, have emerged. The effect is most pronounced around the crossing region ($M_{H^+} \sim 150\,\mathrm{GeV}$). This is expected, since the scalar/pseudo-scalar mixing in H_1 is largest here. For much higher values of M_{H^+}, H_1 is purely a scalar. There can still be a CP-violating effect through its sfermion couplings, though. The latter will be more visible when there is a light sparticle in the loop (a stop, in particular). For $M_{H^+} < 150\,\mathrm{GeV}$ there is still sufficient mixing to have a substantial difference in the BR. But in this region M_{H_1} is also changed by about 10 to 15% between $\phi_\mu = 0°$ and $\phi_\mu = 90°$. We will, however, concentrate on the region $M_{H^+} > 150\,\mathrm{GeV}$, where $M_{H_1} > 115\,\mathrm{GeV}$ for the parameter sets considered. Moreover, the effect of $\phi_\mu \neq 0$ on M_{H_1} in this region is within 1 GeV, which is less than the experimental uncertainty expected at the LHC. In particular, we have learnt that the width and BR of the decay $H_1 \to \gamma\gamma$ are very sensitive to the $\tilde{t}_1$ mass. The effect comes through both a modification of the $H_1 W^+ W^-$ couplings and the presence of a light $\tilde{t}_1$ in the triangle loops of the decay amplitude.

As it is unfeasible to present all the results of our scan, we have picked out a few different discrete choices of the relevant MSSM parameters and plotted width and BR against M_{H^+} for the latter in Figs. 11–18. We choose five representative values between 0° and 180° for the phase of μ.[3] Figure 11 is with $|A_f| = 1.5\,\mathrm{TeV}$, $|\mu| = 1\,\mathrm{TeV}$ and

[3] To aid the reader, through multiple x-axes and labels, we have included the mass of H_1 in each plot corresponding to $M_{H^\pm}$ for the given choice of other MSSM parameters. Besides, in each figure we have zoomed in near and above the aforementioned cross over point at $M_{H^\pm} \approx 150\,\mathrm{GeV}$. Finally, as the BR is the measurable quantity, we dwell on this while only plotting the width for reference.

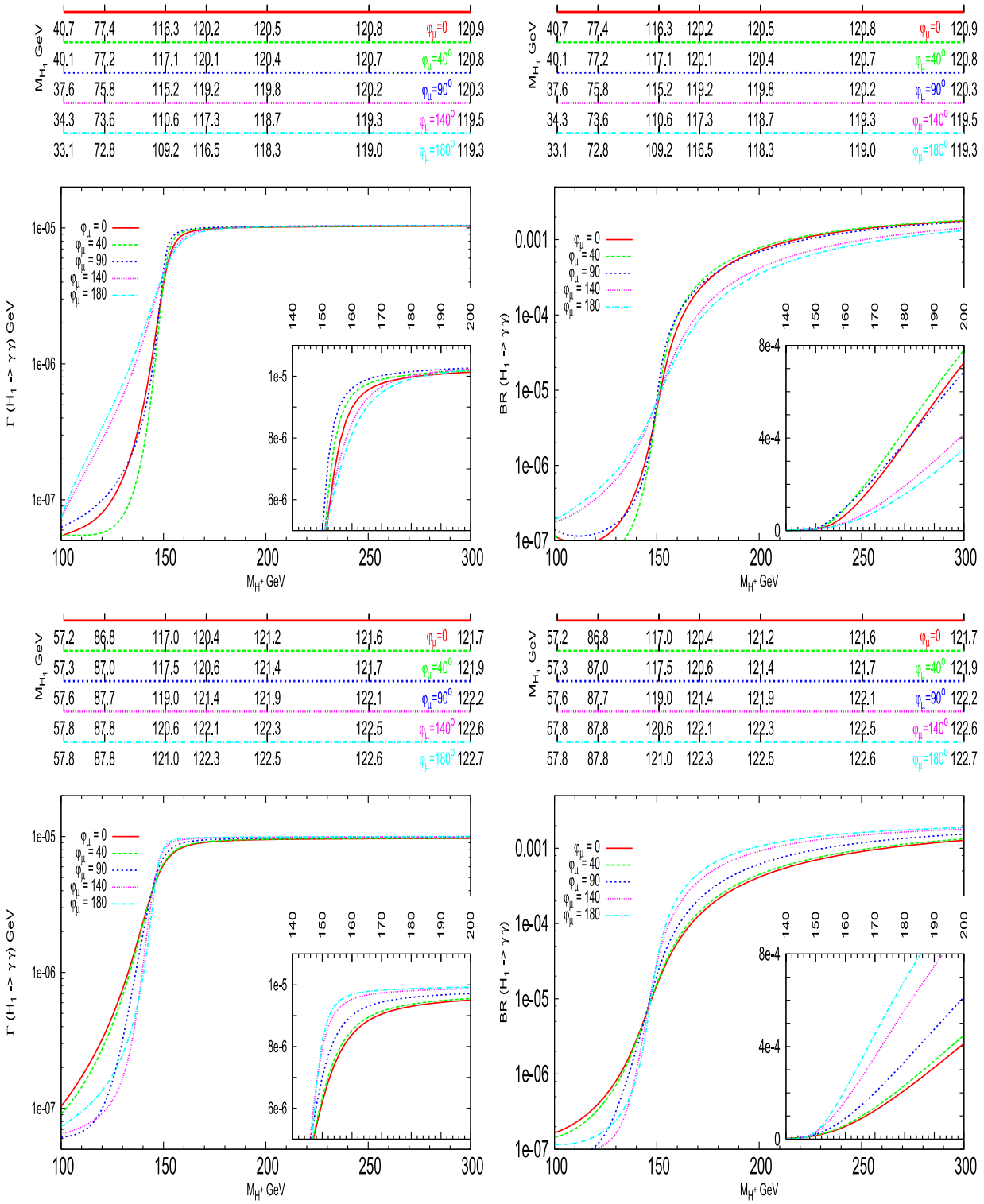

Fig. 11. Width (*left column*) and BR (*right column*) of $H_1 \to \gamma\gamma$ against the input parameter M_{H^+} for $|A_f| = 1.5$ TeV, $|\mu| = 1$ TeV and $\tan\beta = 20$. Values of M_{H_1} corresponding to representative points on M_{H^+} axis are indicated on the *horizontal lines* above separately for the values of ϕ_μ used. The *top row* corresponds to the case with $M_{\tilde{U}_3} = 250$ GeV, while the *bottom one* corresponds to the case with $M_{\tilde{U}_3} = 1$ TeV

$\tan\beta = 20$. Comparing the two cases of $M_{\tilde{U}_3} = 250$ GeV and $M_{\tilde{U}_3} = 1$ TeV, there is a qualitative difference in the sensitivity to ϕ_μ. This is also true for Fig. 12, which assumes $|A_f| = 1.5$ TeV and $\tan\beta = 20$, but the smaller value $|\mu| = 500$ GeV. In the first case there is an increase in the BR over the region $M_{H^+} > 150$ GeV (and a decrease over

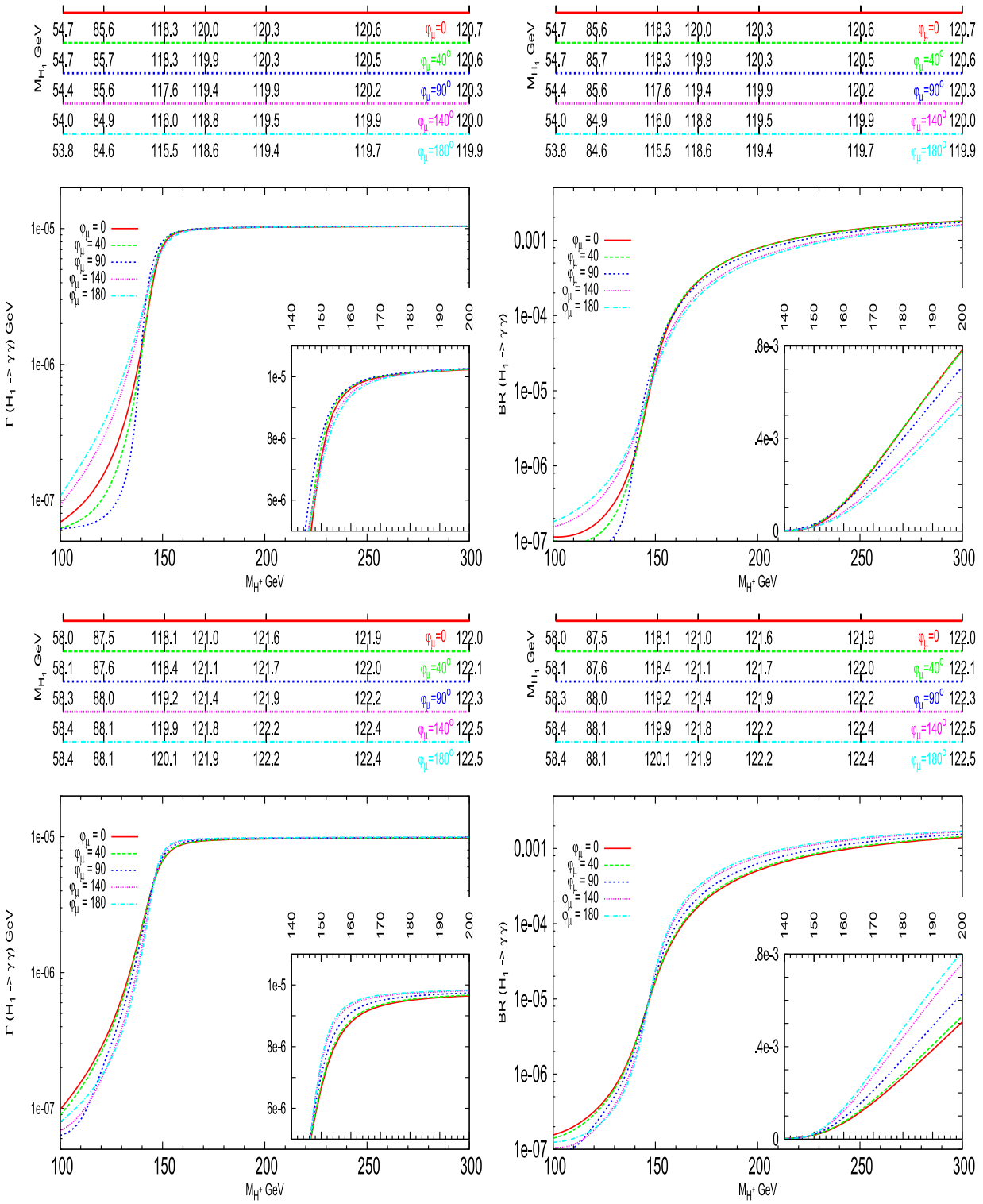

Fig. 12. Similar to Fig. 11, but with $|A_f| = 1.5$ TeV, $|\mu| = 0.5$ TeV and $\tan\beta = 20$

the region $M_{H^+} < 150$ GeV) as ϕ_μ is switched on. This relative change with ϕ_μ is maximised for some value of ϕ_μ around 40°, beyond which the change in BR decreases again to about 50% at $\phi_\mu = 180°$. In the second case there is no such a trend as there is a 50% increase in the BR for $\phi_\mu = 90°$ at $M_{H^+} \sim 200$ GeV and the effect grows larger for $\phi_\mu > 90°$. Other general features are the following. The dependence on ϕ_μ decreases with lower values of $|\mu|$ as seen from Fig. 12. The value of ϕ_μ with maximum BR in the presence of a light $\tilde{t}_1$ decreases compared to the case when $|\mu| = 1$ TeV. In contrast, a smaller value of $|A_f| = 500$ GeV (Figs. 13 and 14) keeps the picture qualitatively the same

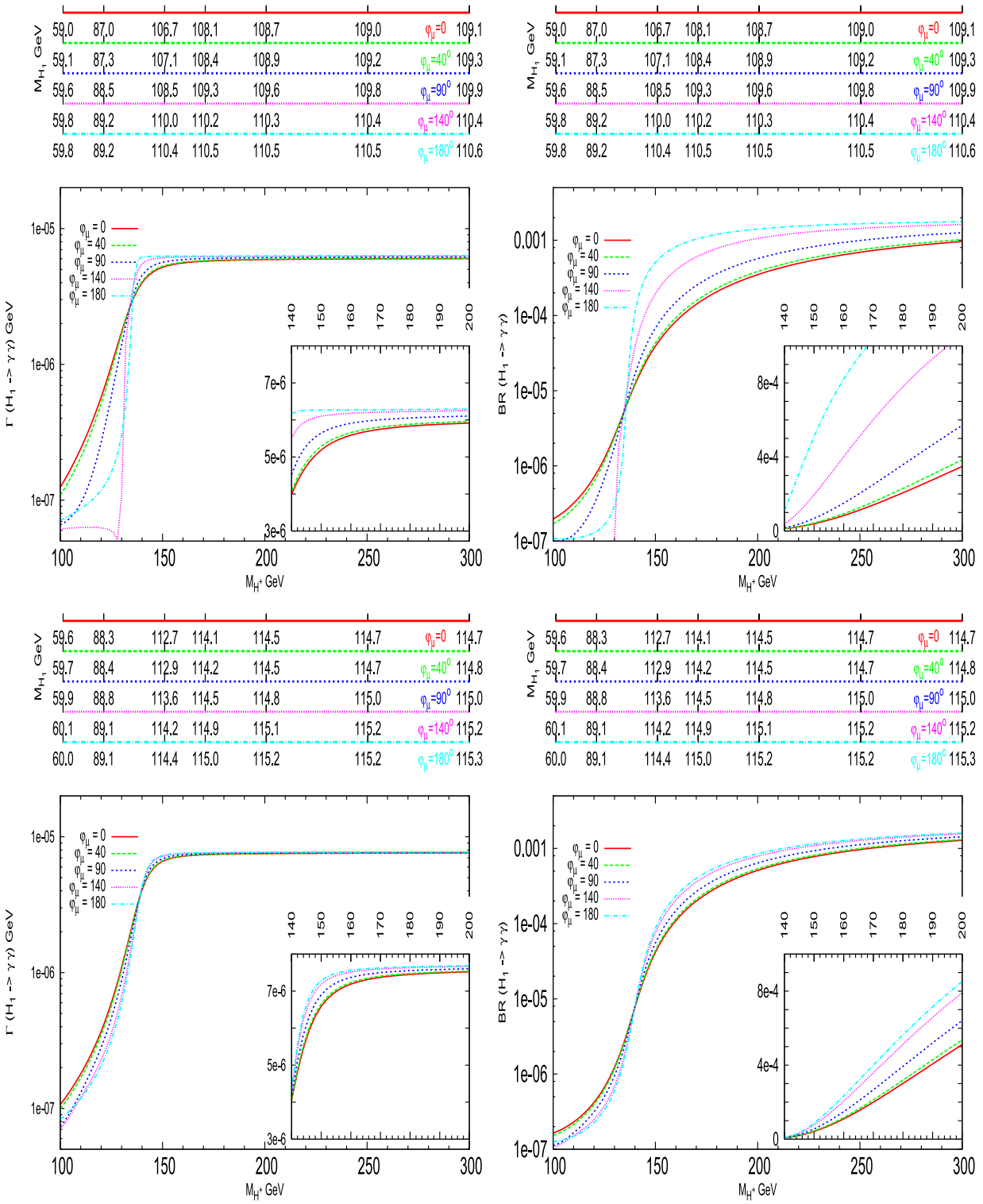

Fig. 13. Similar to Fig. 11, but with $|A_f| = 0.5$ TeV, $|\mu| = 1$ TeV and $\tan\beta = 20$

for the two cases of light and heavy $\tilde{t}_1$: e.g., in the region $M_{H^+} > 150$ GeV, the BR increases with increasing ϕ_μ. But, while in the first case ($M_{\tilde{U}_3} = 250$ GeV) there is a 50% increase for $\phi_\mu = 90°$ at $M_{H^+} = 200$ GeV, in the second case ($M_{\tilde{U}_3} = 1$ TeV) there is an increase of less than 20%. Again, the deviations can be substantially larger for $\phi_\mu > 90°$. The sensitivity of BR($H_1 \to \gamma\gamma$) to ϕ_μ is, however, reduced considerably for lower values of $\tan\beta$, while the qualitative features remain the same, as is illustrated in Figs. 15–18 for $\tan\beta = 5$.

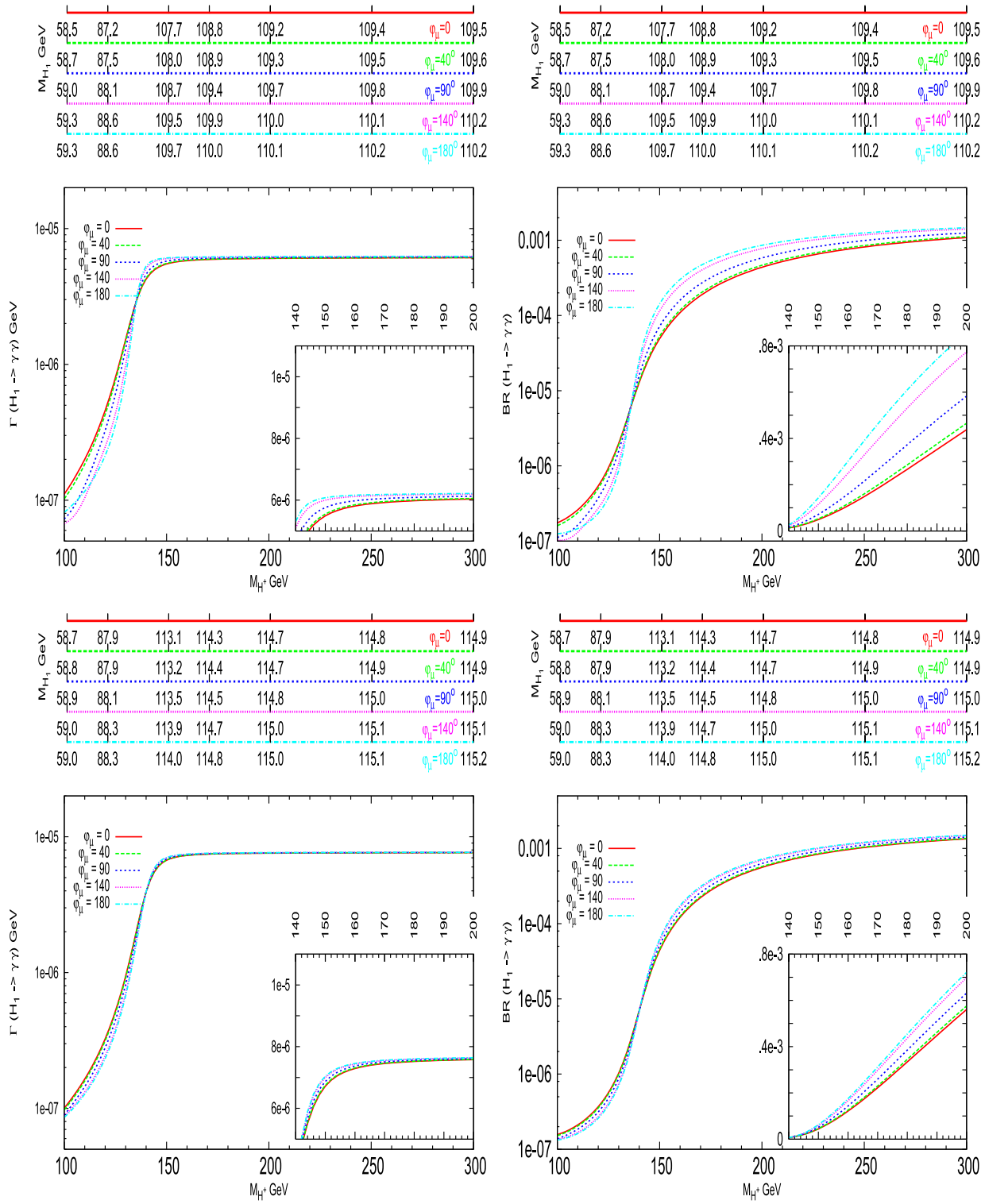

Fig. 14. Similar to Fig. 11, but with $|A_f| = 0.5$ TeV, $|\mu| = 0.5$ TeV and $\tan\beta = 20$

4 Conclusion

In this paper, we have demonstrated that the decay channel $H_1 \to \gamma\gamma$ is particularly suitable to probe the possible presence of CP-violating effects in the MSSM. This mode is in fact not only very sensitive to variations of the coupling $H_1W^+W^-$ pertaining to the dominant SM loop – induced from mixing amongst Higgs states via one-loop effects (as shown in previous literature) – but also to contributions of a light $\tilde{t}_1$ in the triangle loop defining the decay process – which is in fact a tree-level effect induced by a complex μ parameter (while the trilinear coupling A_t is taken real).

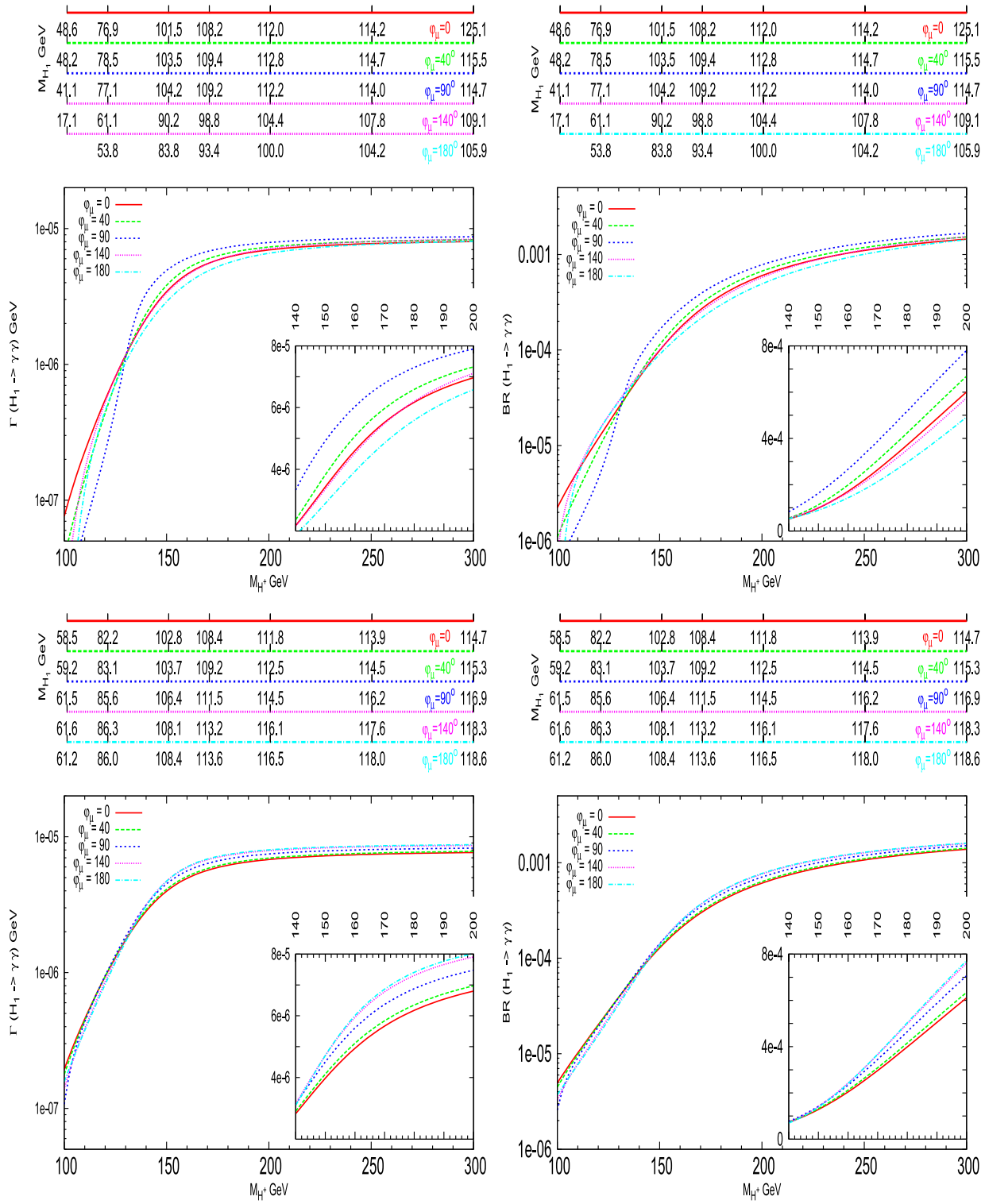

Fig. 15. Similar to Fig. 11, but with $|A_f| = 1.5$ TeV, $|\mu| = 1$ TeV and $\tan\beta = 5$

In particular, our detailed analyses indicate that studies of the di-photon channel of a light Higgs boson (with mass below 130 GeV or so) found at the LHC may eventually enable one to disentangle the CP-violating case from the CP-conserving one, so long as the relevant SUSY parameters entering $H_1 \to \gamma\gamma$ are measured elsewhere. This is not phenomenologically unconceivable, as the $H_1 \to \gamma\gamma$ detection mode requires a very high luminosity, unlike the discovery of those sparticles (and the measurement of their masses and couplings) that enter the Higgs process studied here. Furthermore, while explicit CP violation could affect the mass of the lightest Higgs state of the underlying

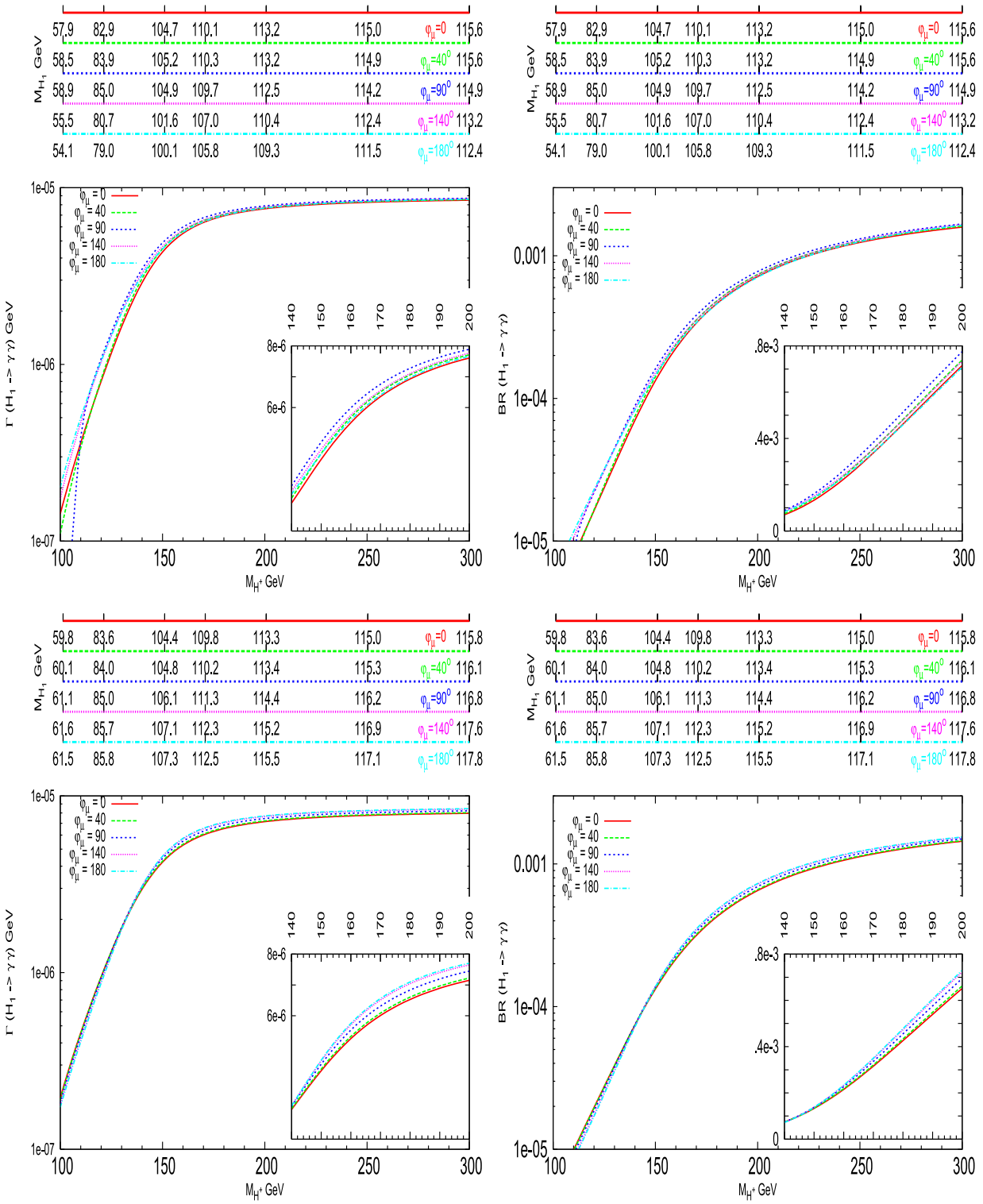

Fig. 16. Similar to Fig. 11, but with $|A_f| = 1.5$ TeV, $|\mu| = 0.5$ TeV and $\tan\beta = 5$

SUSY model, we have restricted ourselves to regions of parameter space where – for an identical choice of all SUSY inputs but ϕ_μ, the only relevant phase in the scenarios considered here – the difference between the M_{H_1} values in the CP-violating case and the CP-conserving one are below the experimental uncertainty on the determination of such a quantity, so that it would not be possible to confirm or disprove the existence of complex parameters in the SUSY Lagrangian by solely isolating a H_1 resonance.

A complete analysis will eventually require one to fold the decay process studied here in the narrow width approximation with propagator effects and the appro-

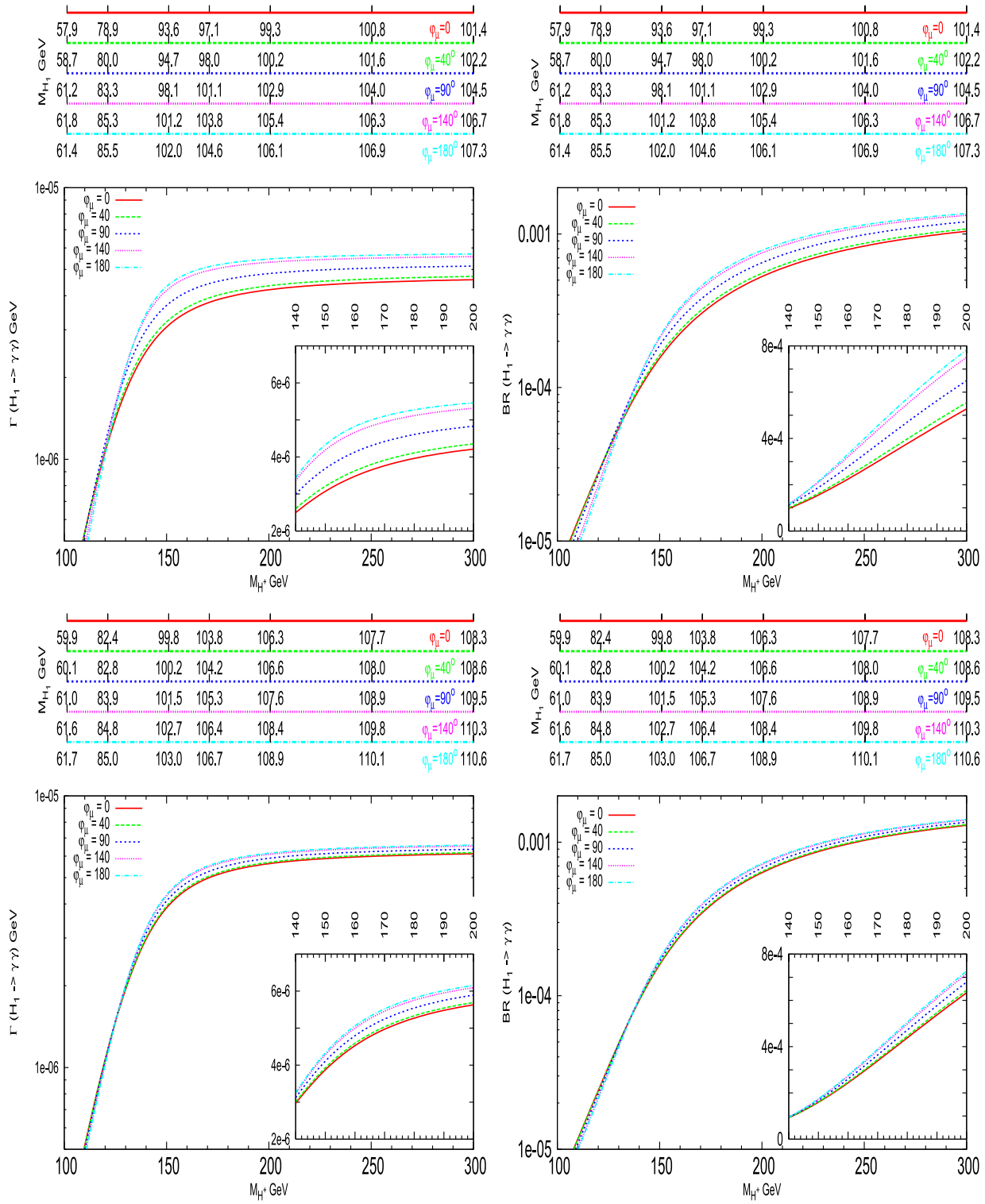

Fig. 17. Similar to Fig. 11, but with $|A_f| = 0.5$ TeV, $|\mu| = 1$ TeV and $\tan\beta = 5$

priate production mode (gluon–gluon fusion and Higgs-strahlung in this case), where similar CP-violating effects may enter. This will be done in a future publication [61]. Finally, as argued in Sect. 1, for the scenario we considered here, with very heavy squarks and vanishing trilinear couplings for the first and second generations, we can evade the EDM constraints on the CP-violating phases. A detailed analysis of this is also deferred to future work.

Acknowledgements. P.P.'s research is supported by the Framework Programme 6 via a Marie Curie International Incoming

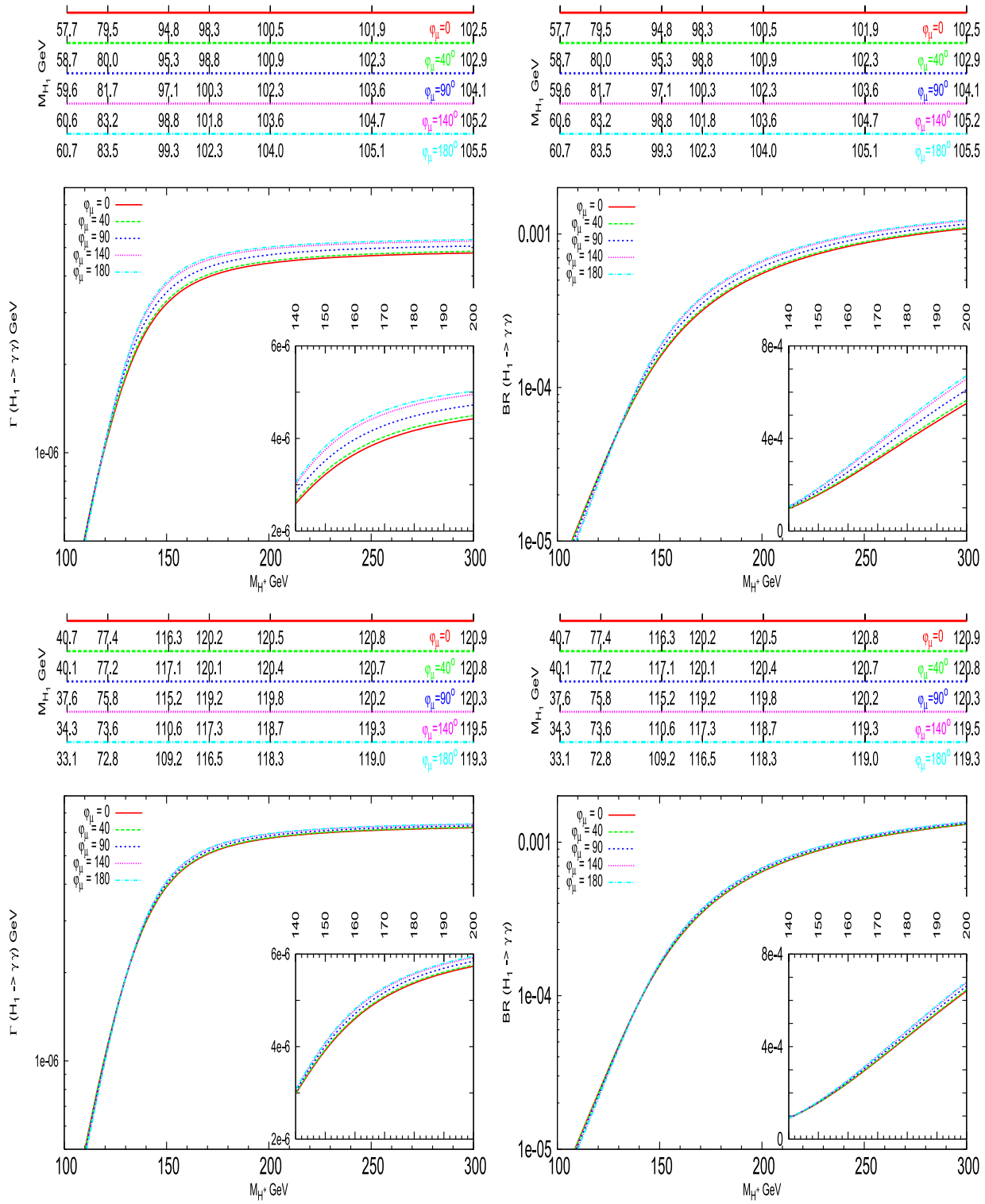

Fig. 18. Similar to Fig. 11, but with $|A_f| = 0.5$ TeV, $|\mu| = 0.5$ TeV and $\tan\beta = 5$

Fellowship, contract number MIF1-CT-2004-002989. This research has been partially financed by the NATO Collaborative Linkage Grant no. PST.CLG.980066. SM thanks the RTN European Programme MRTN-CT-2006-035505 (HEPTOOLS, Tools and Precision Calculations for Physics Discoveries at Colliders) for partial financial support.

References

1. A. Djouadi, hep-ph/0503172
2. A. Djouadi, hep-ph/0503173
3. J.F. Gunion, H.E. Haber, G. Kane, S. Dawson, The Higgs Hunter's Guide (Addison-Wesley, Reading, MA, 1990)

4. N. Maekawa, Phys. Lett. B **282**, 387 (1992)
5. A. Pilaftsis, Phys. Lett. B **435**, 88 (1998)
6. H. Georgi, A. Pais, Phys. Rev. D **10**, 1246 (1974)
7. A. Pomarol, Phys. Lett. B **287**, 331 (1992)
8. N. Haba, Phys. Lett. B **398**, 305 (1997)
9. O.C.W. Kong, F.L. Lin, Phys. Lett. B **418**, 217 (1998)
10. A. Pilaftsis, C.E.M. Wagner, Nucl. Phys. B **553**, 3 (1999)
11. M. Dugan, B. Grinstein, L. Hall, Nucl. Phys. B **255**, 413 (1985)
12. D. Chang, W.Y. Keung, A. Pilaftsis, Phys. Rev. Lett. **82**, 900 (1999)
13. P. Nath, Phys. Rev. Lett. B **66**, 2565 (1991)
14. Y. Kuzikuri, N. Oshimo, Phys. Rev. D **45**, 1806 (1992)
15. Y. Kuzikuri, N. Oshimo, Phys. Rev. D **46**, 3025 (1992)
16. S. Abel, S. Khalil, O. Lebedev, Nucl. Phys. B **606**, 151 (2001)
17. K.A. Olive, M. Pospelov, A. Ritz, Y. Santoso, Phys. Rev. D **72**, 075 001 (2005)
18. S. Abel, O. Lebedev, JHEP **0601**, 133 (2006)
19. T. Ibrahim, P. Nath, Phys. Lett. B **418**, 98 (1998)
20. T. Ibrahim, P. Nath, Phys. Rev. D **57**, 478 (1998)
21. T. Ibrahim, P. Nath, Phys. Rev. D **58**, 019 901 (1998)
22. T. Falk, K.A. Olive, Phys. Lett. B **439**, 71 (1998)
23. M. Brhlik, G.J. Good, G.L. Kane, Phys. Rev. D **59**, 115 004 (1999)
24. S. Pokorski, J. Rosiek, C.A. Savoy, Nucl. Phys. B **570**, 81 (2000)
25. S. Yaser Ayazi, Y. Farzan, Phys. Rev. D **74**, 055 008 (2006)
26. A. Pilaftsis, Nucl. Phys. B **644**, 263 (2002)
27. S. Dimopoulos, G.F. Giudice, Phys. Lett. B **357**, 573 (1995)
28. A. Cohen, D.B. Kaplan, A.E. Nelson, Phys. Lett. B **388**, 588 (1996)
29. A. Pamarol, D. Tommasini, Nucl. Phys. B **488**, 3 (1996)
30. A. Bartl, W. Majerotto, W. Porod, D. Wyler, Phys. Rev. D **68**, 053 005 (2003)
31. S.Y. Choi, J.S. Lee, Phys. Rev. D **61**, 015 003 (2000)
32. S.Y. Choi, J.S. Lee, Phys. Rev. D **61**, 115 002 (2000)
33. S.Y. Choi, J.S. Lee, Phys. Rev. D **62**, 036 005 (2000)
34. S.Y. Choi, K. Hagiwara, J.S. Lee, Phys. Rev. D **64**, 032 004 (2001)
35. S.Y. Choi, M. Drees, J.S. Lee, J. Song, Eur. Phys. J. C **25**, 307 (2002)
36. M. Carena, J. Ellis, A. Pilaftsis, C.E.M. Wagner, Phys. Lett. B **495**, 155 (2000)
37. M. Carena, J. Ellis, S. Mrenna, A. Pilaftsis, C.E.M. Wagner, Nucl. Phys. B **659**, 145 (2003)
38. J. Ellis, J.S. Lee, A. Pilaftsis, Phys. Rev. D **70**, 075 010 (2004)
39. J. Ellis, J.S. Lee, A. Pilaftsis, Mod. Phys. Lett. A **21**, 1405 (2006)
40. S.Y. Choi, M. Drees, B. Gaissmaier, Phys. Rev. D **70**, 014 010 (2004)
41. A. Bartl, S. Hesselbach, K. Hidaka, T. Kernreiter, W. Porod, Phys. Lett. B **573**, 153 (2003)
42. A. Bartl, S. Hesselbach, K. Hidaka, T. Kernreiter, W. Porod, Phys. Rev. D **70**, 035 003 (2004)
43. A. Bartl, H. Fraas, S. Hesselbach, K. Hohenwarter-Sodek, G.A. Moortgat-Pick, JHEP **0408**, 038 (2004)
44. A. Bartl, H. Fraas, S. Hesselbach, K. Hohenwarter-Sodek, T. Kernreiter, G. Moortgat-Pick, JHEP **0601**, 170 (2006)
45. A. Bartl, H. Fraas, S. Hesselbach, K. Hohenwarter-Sodek, T. Kernreiter, G. Moortgat-Pick, Eur. Phys. J. C **51**, 149 (2007)
46. ATLAS Collaboration, ATLAS Detector and Physics Performance: Technical Design Report, 2, CERN-LHCC-99-015 (1999)
47. CMS Collaboration, CMS Physics: Technical Design Report v.2: Physics Performance, CERN-LHCC-2006-021 (2006)
48. A. Dedes, S. Moretti, Phys. Rev. Lett. **84**, 22 (2000)
49. A. Dedes, S. Moretti, Nucl. Phys. B **576**, 29 (2000)
50. M. Carena, J. Ellis, A. Pilaftsis, C.E.M. Wagner, Nucl. Phys. B **586**, 92 (2000)
51. S.Y. Choi. K. Hagiwara, J.S. Lee, Phys. Lett. B **529**, 212 (2002)
52. A. Arhrib, D.K. Ghosh, O.C.W. Kong, Phys. Lett. B **537**, 217 (2002)
53. S.Y. Choi, M. Drees, B. Gaissmaier, Phys. Rev. D **70**, 014 010 (2004)
54. D.A. Demir, Phys. Rev. D **60**, 055 006 (1999)
55. D.K. Ghosh, S. Moretti, Eur. Phys. J. C **42**, 341 (2005)
56. D.K. Ghosh, R.M. Godbole, D.P. Roy, Phys. Lett. B **628**, 131 (2005)
57. R. Godbole, D.J. Miller, S. Moretti, M. Muhlleitner, hep-ph/0608079
58. R. Godbole, D.J. Miller, S. Moretti, M. Muhlleitner, hep-ph/0602198
59. A. Skjold, P. Osland, Phys. Lett. B **329**, 305 (1994)
60. S. Moretti, S. Munir, P. Poulose, Phys. Lett. B **649**, 206 (2007)
61. S. Hesselbach, S. Moretti, S. Munir, P. Poulose, in preparation
62. S. Heinemeyer, Int. J. Mod. Phys. A **21**, 2659 (2006)
63. M. Frank, T. Hahn, S. Heinemeyer, W. Hollik, H. Rzehak, G. Weiglein, hep-ph/0611326
64. J.S. Lee et al., Comput. Phys. Commun. **156**, 283 (2004)
65. M. Carena, J.R. Ellis, A. Pilaftsis, C.E.M. Wagner, Nucl. Phys. B **625**, 345 (2002)
66. B. Ananthanarayan, G. Lazarides, Q. Shafi, Phys. Rev. D **44**, 1613 (1991)
67. R. Hemphling, Phys. Rev. D **49**, 6168 (1994)
68. L. Hall, R. Rattazzi, U. Sarid, Phys. Rev. D **50**, 7048 (1994)
69. M. Carena, M. Olechowski, S. Pokorski, C.E.M. Wagner, Nucl. Phys. B **426**, 269 (1994)
70. D. Pierce, J. Bagger, K. Matchev, R. Zhang, Nucl. Phys. B **491**, 3 (1997)
71. J.A. Coarasa, R.A. Jimenez, J. Sola, Phys. Lett. B **389**, 312 (1996)
72. R.A. Jimenez, J. Sola, Phys. Lett. B **389**, 53 (1996)
73. K.T. Matchev, D.M. Pierce, Phys. Lett. B **445**, 331 (1999)
74. P.H. Chankowski, J. Ellis, M. Olechowski, S. Pokorski, Nucl. Phys. B **544**, 39 (1999)
75. K.S. Babu, C. Kolda, Phys. Lett. B **451**, 77 (1999)